University of Arkansas, Fayetteville

ScholarWorks@UARK

Graduate Theses and Dissertations

8-2014

Characterizing Nanoparticle Size by Dynamic Light Scattering Technique (DLS)

Marzia Zaman
University of Arkansas, Fayetteville

Follow this and additional works at: https://scholarworks.uark.edu/etd

Part of the Nanoscience and Nanotechnology Commons, and the Optics Commons

Characterizing Nanoparticle Size by Dynamic Light Scattering Technique (DLS)

Characterizing Nanoparticle Size by Dynamic Light Scattering Technique (DLS)

A thesis submitted in partial fulfillment
of the requirements for the degree of
Master of Science in Microelectronics-Photonics

By

Marzia Zaman
University of Dhaka
Bachelor of Science in Applied Physics Electronics and Communication Engineering, 2010

August 2014
University of Arkansas

This thesis is approved for recommendation to the Graduate Council.

_____
Dr. Surendra P. Singh
Thesis Director

_____
Dr. Omar Manasreh
Committee Member

_____
Dr. Jingyi Chen
Committee Member

_____
Prof. Ken Vickers
Ex-Officio Member

The following signatories attest that all software used in this thesis was legally licensed for use by Marzia Zaman for research purposes and publication.

_____   _____

Ms. Marzia Zaman, Student   Dr. Surendra P. Singh, Thesis Director

This thesis was submitted to http://www.turnitin.com for plagiarism review by the TurnItIn Company's software. The signatories have examined the report on this thesis that was returned by TurnItIn and attest that, in their opinion, the items highlighted by the software are incidental to common usage and are not plagiarized material.

_____   _____

Prof. Ken Vickers, Program Director   Dr. Surendra P. Singh, Thesis Director

Abstract

The Dynamic Light Scattering Technique was used to determine the size, shape and diffusion coefficient of nanoparticle. The intensity auto correlation functions of light scattered by particles in a solution were measured by using a photomultiplier tube and analyzed to get the relaxation rates for decay of intensity correlations, which correspond to the diffusion constants pertaining to the motion of the particle. In the case of nanorods there are two types of motion - translational and rotational. By dis-entangling the relaxation rates, corresponding to these two types of motion, the shape and size of nanoparticle could be characterized. These experiments, though limited in scope, demonstrate the promise of dynamical light scattering as an inexpensive and convenient technique for characterizing regular shaped nano-particles in a fluid medium.

Acknowledgements

I would like to thank almighty Allah for everything and giving me strength to finish this Thesis.

I would like to express my deepest gratitude to my thesis committee chair, Dr. Surendra Singh who has guided me all through my research and thesis writing. Without his guidance and continuous help, I would not able to finish this thesis.

I would like to thank Professor Ken Vickers for his help whenever I needed it despite his busy schedule.

I also want to thank my committee members for their feedback on my thesis.

Last but not the least, I want to thank my family and friends for their constant help and support in my research and thesis.

Dedication

I would like to dedicate my thesis to my microEP fellows

Table of contents

List of figures

List of tables

Chapter 1

Introduction

1.1 Motivation:

Nanoparticles have a wide range of applications including those in the fields of drug delivery, cell and molecular biology, biomedical engineering, electronic devices. In these and, any other field of science and technology, nanoparticles bring new capabilities. The properties of nanoparticles change with their size and shape. This thesis is about a technique to determine their size and shape by measuring their translational and rotational diffusion coefficients in a fluid medium.

There are several other techniques such as the Transmission Electron Microscopy (TEM) and the Scanning Electron Microscopy (SEM), which are used to determine the size of nanoparticles. In TEM technique high voltage electron beam from an electron gun is transmitted through the sample to be measured and according to the intensity of the transmitted electron beam, the image of sample is constructed on a fluorescent screen in the microscope or camera. The SEM technique is similar to the TEM except that it uses scattered electron beam to construct the image instead of the transmitted electron beam.

The TEM and SEM systems are expensive because of their sophisticated electronics and high maintenance costs. Besides the cost of these techniques, these systems are not user friendly because an expert is needed to operate the system. So, there is a need for an alternative and inexpensive system for sizing nanoparticles. The dynamic light scattering technique is a relatively inexpensive and a convenient technique to solve this problem.

1.2 Light scattering:

In light scattering technique a vertically polarized coherent light is shined on a nanoparticle sample. In nanoparticle-light interaction, the scattered light contains information about the particles. If the particles are small in comparison to the wavelength of the light, each particle can be treated as a dipole, which radiates light, which appears as scattered light. The intensity of the scattered light depends on different features of the particle. This scattered light can be analyzed to characterize the particle properties.

There are two approaches to analyzing the particles: static light scattering (SLS) and dynamic light scattering (DLS). In static light scattering technique, the time averaged intensity of scattered light at different angle is used to measure the molecular weight, radius of gyration, the second virial coefficient. On the other hand, in dynamic light scattering technique, the intensity of scattered light is recorded for some time interval and by analyzing the auto correlation function, the size, diffusion coefficient, and their temperature dependence can be determined.

1.3 History of dynamic light scattering technique:

The idea of scattered light was first introduced in the early 19th century by physicist Tyndall in his so-called Tyndall effect experiment [1]. In this experiment he showed that the scattered light intensity depends on the frequency of incident light and that shorter wavelength light can be used to measure the colloid particles in a suspension. These particles were much larger compared to the size of nanoparticles.

Later, another famous physicist Lord Rayleigh demonstrated the use of light scattering for determining the size of smaller particle [1]. The Rayleigh effect is applicable when the size of

the particle is comparable to the wavelength of the scattered light. In both Tyndall and Rayleigh effects, the frequency or the wavelength of the light is an important parameter.

The photon correlations of the intensity of the scattered light were first demonstrated in 1956. The effect is called Hanbury-Brown Twiss effect [1]. This technique is used in astronomy. Till that time the incident light which was used for different scattering experiments was produced from thermal sources

With the discovery of laser light in 1960, laser light scattering experiments were carried out by many different scientists. In 1966, the spectral distribution of scattered laser light from fluid was examined by Mountain [1]. The experiments based on laser light spectroscopy were done by Cummins [1].

A complete book on laser light scattering technique was published in 1974 by Chu [1] where different types of light scattering experiments were discussed. In 1972, Pecora showed the quasi-elastic laser light scattering from macromolecule. Later in 1974, a complete book of dynamic light scattering technique was published by Bruce Berne and Robert Pecora [1]. This book describes the use of Dynamic light scattering technique to characterize isotropic and anisotropic particle, interaction of particle in different solution etc. In this book both polarized and depolarized dynamic light scattering technique have been discussed.

The use of Laser light scattering in the field of biomedical was initiated in 1980 by Sattelle [1]. In another updated study by Chu, the laser light technology was used for polymer particle characterization in 1985 [1]. Now-a-days, different scientists have been working on light scattering technique to find new application of it. The protein-protein interaction is one of those very important applications of this technique that has been done recently [1].

1.4 Thesis overview:

This thesis demonstrates the use of dynamic light scattering technique for measuring the size of nanorod shaped particles. The essential procedure outlined by Robert Pecora in his book Dynamic Light Scattering technique [1] was followed. The sizes of three different samples were measured. Two of those samples were bare gold nanorods of different sizes and the third one was made of nanorods of Gold Copper alloy ($AuCu_3$). A polystyrene nanosphere sample was also measured to calibrate the apparatus. Different steps involved in these measurements are described in detail in different chapters.

In the second chapter the theoretical basis of the experiments is presented. As a first step the relation between scattered light intensity and the polarizability of the nano particle is derived. The theoretical models for both nano-sphere and nano-rod particles have been considered. In case of nano-spheres the diffusion of nano particle is only for translational movement. So the intensity of the scattered light is only related to translational diffusion. On the other hand, if the particle is a nano-rod, there will be both translational and rotational movement due to its anisotropic shape (different diameter and length). The model for light scattered by a nanorod particle involves its polarizability tensor, which, in turn, is related to translational and diffusional movement.

In the third chapter, the description of the experimental set up for this experiment is given. The main part of this set up is a scattering chamber mounted on a goniometer. A vertically polarized He:Ne laser beam is collimated and focused by a set of lenses into the center of the scattering chamber that holds the scattering sample. Another set of lenses and apertures collect the scattered light, which is then guided to a photomultiplier tube. The output from the photomultiplier is used to measure the auto correlation function of the scattered light intensity.

The analysis of the measured correlation function is carried out by the light scattering software. A temperature controller is also included in the set up to record measurements at different temperatures by changing the sample temperature.

In the fourth chapter, the data analysis of the autocorrelation function of the scattered light is given. According to the theoretical models described in Chapter 2, the size of nanorods and nanospheres can be determined through data analysis of the measured correlation functions. Two different approaches of data analysis were used to determine two different particle samples. The cumulant data fitting is used for nanospheres. In the case of nanorods, double exponential fitting is needed due to two different types of motion - translational and rotational diffusion. Consequently, there will be at least two different relaxations rate in the auto correlation of the scattered light.

The thesis ends by summarizing the principal findings and outlining principal advantages and limitations of light scattering technique for nano-particle characterization.

Chapter 2

Theory

The dynamic light scattering technique is used to characterize particles by their size, molecular weight, shape, diffusion coefficient, and angular and temperature dependence of these characteristics by analyzing the properties of light scattered by the particles. In this technique laser light is shined on particles in a solution and the scattered light from the solution is analyzed and information about the particles is extracted from the data by using different models of light scattering. In general, the information about size has to be interpreted with care. Only for spherical particles can one unambiguously assign a meaning to the size information extracted from light scattering data. For anisotropic shapes, the size is an "average" of particle dimensions in different orientations. For anisotropic particles, scattering is expected to be polarization dependent, for the particles not only undergo translational diffusion but also change their orientation (rotational diffusion) and depending on the orientation of the particle, the induced dipole moment and, therefore, the polarization and strength of scattered light will be different. This suggests that polarization dependence of scattered light may be used for extracting shape information. This is demonstrated by carrying out measurements on three different samples of nano-particles of cylindrical shape. As a reference the measurements on spherical shape particles is also included. The theoretical model proposed by Bruce J. Berne and Robert Pecora in the book "Dynamic Light Scattering" [2], is followed to interpret the measurements. In the following the models for light scattering from spherical and nanorod particles models and derive corresponding expressions for spectral density of scattered light and their dependence on the polarizability are summerized.

2.1 Spectral density of scattered light from dielectric permittivity fluctuations

There are two different models for spherical and nanorod particle sizing using light scattering. These models are based on scattered light analysis in terms of different polarization tensors. In this section, the theory is began by considering the general geometry of scattered light as shown in Fig (1).

A beam of light propagating in a direction characterized by the propagation vector $\mathbf{k_i}$ is incident on a sample of particles suspended in a liquid medium. The electric field of the incident light is written as

$$\mathbf{E_i}(r,t) = \mathbf{n_i} E_o \exp i(\mathbf{k_i}.\mathbf{r} - \omega_i t) \tag{2.1}$$

where, according to Fig (1), $\mathbf{n_i}$ is the polarization of the incident light wave, E_o is the amplitude of the electric field, $\mathbf{k_i}$ is the wave vector in the direction of the propagation of incident light wave and ω_i is the angular frequency of the incident wave. The refractive index of the medium is n. The dielectric constant of the medium to be analyzed is written as

$$\boldsymbol{\varepsilon}(\mathbf{r},t) = \varepsilon_o \boldsymbol{\sigma} + \delta\boldsymbol{\varepsilon}(\mathbf{r},t), \tag{2.2}$$

where the $\delta\boldsymbol{\varepsilon}(\mathbf{r},t)$ is the dielectric constant fluctuation tensor at position r and time t and $\boldsymbol{\sigma}$ is the second rank unit tensor. The dielectric constant fluctuations arise because of the local particle density fluctuations and the interaction between incident light and the particle. These dielectric fluctuations carry the information about the particles scattering the light. The spatial Fourier transform of the dielectric fluctuation $\delta\boldsymbol{\varepsilon}(\mathbf{r},t)$ is

$$\delta\boldsymbol{\varepsilon}(\mathbf{q},t) = \int_V d^3r \, \exp(i\mathbf{q}.\mathbf{r}) \delta\boldsymbol{\varepsilon}(\mathbf{r},t) \tag{2.3}$$
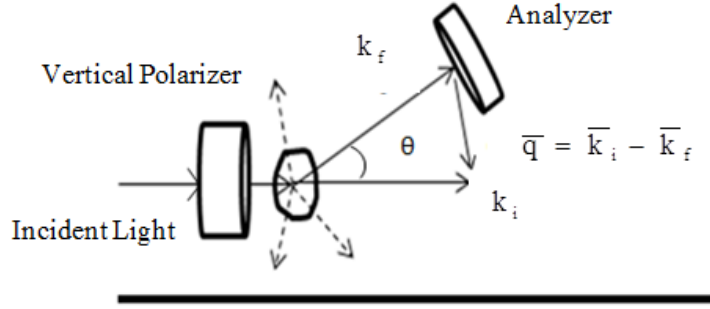
Fig (2.1): Light scattering geometry for a particle to be analyzed

The incident light is scattered in all directions when it passes through the dielectric medium [See Fig. 2.1]. The observer is at a distance R from the origin in a direction making angle θ with the direction of the incident light wave. The polarization of the collected scattered light is $\mathbf{n_f}$, the wave vector of it is $\mathbf{k_f}$, which indicates the propagation direction of the collected scattered light, and the angular frequency is ω_f. . The time and position dependent scattered electric field is then [1]

$$E_s(R,t) = \frac{A_o}{4\pi R \varepsilon_o} \exp(ik_f R) \int_v d^3 r \exp i(\mathbf{q.r} - i\omega_i t) \mathbf{n_f}.[\mathbf{k_f} \times (\mathbf{k_f} \times (\delta\varepsilon(\mathbf{r},t).\mathbf{n_i}))]. \qquad (2.4)$$

where A_o the amplitude of the scattered electric field, $\mathbf{q} = \mathbf{k_i} - \mathbf{k_f}$. is the difference between incident and scattering wave vector which is called momentum transfer wave vecto According to Fig (2.1), $q = 2k_i \sin\left(\frac{\theta}{2}\right)$, where we have assumed that, $\mathbf{k_i} \approx \mathbf{k_f}$. By using equation 3 the term

$\int_v d^3 r \exp i \mathbf{q.r} \, \delta\varepsilon(\mathbf{r},t)$ in equation (2.4) can be replace by $\delta\varepsilon(\mathbf{q},t)$ which is the Fourier tnsform of

$\delta\varepsilon(\mathbf{r},t)$. The scattered electric field then becomes,

$$E_s(R,t) = \frac{A_o}{4\pi R \varepsilon_o} \exp i\left(k_f R - i\omega_i t\right)\{\mathbf{n_f}.[\mathbf{k_f} \times (\mathbf{k_f} \times (\delta\varepsilon(\mathbf{q},t).\mathbf{n_i}))]\}$$

$$= \frac{-k_f^2 A_o}{4\pi R \varepsilon_o} \exp i\left(k_f R - \omega_i t\right)\left[\mathbf{n_f}.(\delta\varepsilon(\mathbf{q},t).\mathbf{n_i})\right] \qquad (2.5)$$

The term $\mathbf{n_f}.(\delta\varepsilon(\mathbf{q},t).\mathbf{n_i})$ is the component of dielectric fluctuation tensor in the direction of the initial polarization $\mathbf{n_i}$ and the final polarization $\mathbf{n_f}$. This component is denoted by $\delta\varepsilon_{if}(\mathbf{q},t)$.

The time correlation function of the electric field of the scattered light is

$$< E_s^*(R,0)E_s(R,t) >= \frac{k_f^4 |A_o|^2}{16\pi^2 R^2 \varepsilon_o^2} \left\langle \delta\varepsilon_{if}(\mathbf{q},0)\delta\varepsilon_{if}(\mathbf{q},t)\right\rangle \exp(-i\omega_i t), \qquad (2.6)$$

where $E_s^*(R,0)$ the complex conjugate of $E_s(R,0)$. The spectral density can be measured from the scattered electric field through its time correlation.

$$I_{if}(\mathbf{q},\omega_f,\mathbf{R}) = \left[\frac{B_o k_f^4}{16\pi^2 R^2 \varepsilon_o^2}\right]\frac{1}{2\pi}\int_{-\infty}^{+\infty}dt \left\langle \delta\varepsilon_{if}(\mathbf{q},0)\delta\varepsilon_{if}(\mathbf{q},t)\right\rangle \exp i\left(\omega_f - \omega_i t\right) \qquad (2.7)$$

where $B_o = |A_o|^2$. The proportionality constant $\left[\dfrac{B_o k_f^4}{16\pi^2 R^2 \varepsilon_o^2}\right]$ can be written as C, which depends on the wavelength of the scattered light (as well as the incident light since there is negligible change in wavelength of scattered light).

Note that the spectral density of scattered light is larger for shorter wavelengths than for longer wavelengths. The particles to be studied have different absorbance at different wavelengths. So there is an optimum wavelength where absorption will be less but the spectral density of scattered light will still be significant. The position of the observer R also affects the

9

spectral density. The larger R gives smaller spectral density and since scattering has angular dependence, the angular position will also impact the measured spectral density.

From Eq. (2.7), it is seen that the spectral density of the light scattered at the detector is proportional to the dielectric constant fluctuations

$$\delta \mathbf{I}_{\mathbf{if}}^{\varepsilon}(\mathbf{q},\omega) = \frac{1}{2\pi} \int_{-\infty}^{+\infty} dt \left\langle \delta \varepsilon_{if}(\mathbf{q},0) \delta \varepsilon_{if}(\mathbf{q},t) \right\rangle \exp i \left(\omega_f t - \omega_i t \right), \qquad (2.8)$$

where $\left\langle \delta \varepsilon_{if}(\mathbf{q},0) \delta \varepsilon_{if}(\mathbf{q},t) \right\rangle$ is called the autocorrelation function of the dielectric constant fluctuation $\delta \varepsilon_{if}(\mathbf{q},t)$, which carries information about the size and shape of the particle.

2.2 Spectral density from molecular polarizability

Spectral density can be related to molecular polarizability. The incident light induces a time varying dipole moment that can be written as $\mu(t) = \boldsymbol{\alpha}.\mathbf{E}(t)$, where $\mathbf{E}(t)$ is the electric field of the incident light and $\boldsymbol{\alpha}$ is the polarizability tensor of the molecule to be characterized. This time varying dipole moment causes scattered light. The electric field of this scattered light is proportional to $\alpha_{if}(t) \exp(i\mathbf{q}.\mathbf{r}(t))$, where $\alpha_{if}(t) = \mathbf{n_f}.\boldsymbol{\alpha}(t).\mathbf{n_i}$, which is called the component of the molecular polarizability tensor components along the polarization directions of the incident and scattered light $\mathbf{n_i}$ and $\mathbf{n_f}$. It varies with time because the particle rotates and vibrates in time.

In a dilute solution, the particles are distant enough from each other that they can be assumed to radiate independently. So the total scattered field will be the superposition of the

fields of scattered light by individual particles. The total Fourier spectral density of the scattered

field is proportional to the $\mathbf{I}^{\alpha}_{if}(\mathbf{q}, \omega) = \dfrac{1}{2\pi} \displaystyle\int\limits_{-\infty}^{+\infty} dt \exp i\left(\omega_f t - \omega_i t\right) \mathbf{I}^{\alpha}_{if}(\mathbf{q}, t)$, where

$$\mathbf{I}^{\alpha}_{if}(\mathbf{q}, t) = \left\langle \delta\alpha^{*}_{if}(\mathbf{q}, 0)\delta\alpha_{if}(\mathbf{q}, t) \right\rangle \tag{2.9}$$

and
$$\delta\alpha_{if}(\mathbf{q}, t) = \sum_{j=1}^{N} \alpha^{j}_{if}(t)\exp\left(i\mathbf{q}.\mathbf{r}(t)\right) \tag{2.10}$$

This is the Fourier component of the polarizability tensor.

2.3 Polarization state dependence of dielectric fluctuation

Depending on the incident and scattered light polarization, there are four different types of dielectric constant or polarizability fluctuations. Different particle models differ because of this polarization dependence of dielectric constant or polarizability. For example, for spherical particles, if both the incident and scattered light are either vertically or horizontally polarized, there are different expressions for the dielectric fluctuation tensor:

1. If both incident and scattered lights are vertically polarized, the dielectric fluctuation depends on the $\delta\varepsilon_{zz}(\mathbf{q}, t)$ component:

$$\delta\varepsilon_{VV}(\mathbf{q}, t) = \delta\varepsilon_{ZZ}(\mathbf{q}, t). \tag{2.11}$$

2. If the incident light is vertically polarized and the scattered light is horizontally polarized, the dielectric fluctuation depends on the $\delta\varepsilon_{ZY}(\mathbf{q}, t)$ component:

$$\delta\varepsilon_{VH}(\mathbf{q}, t) = \delta\varepsilon_{ZY}(\mathbf{q}, t). \tag{2.12}$$

11

3. If the incident light is horizontally polarized and the scattered lights are vertically polarized, the dielectric fluctuation depends on $\delta\varepsilon_{XZ}(\mathbf{q},t)$ and $\delta\varepsilon_{YZ}(\mathbf{q},t)$ components and the scattering angle θ:

$$\delta\varepsilon_{HV}(\mathbf{q},t) = \delta\varepsilon_{XZ}(\mathbf{q},t)\sin\theta + \delta\varepsilon_{YZ}(\mathbf{q},t)\cos\theta. \qquad (2.13)$$

4. If both the incident and scattered lights are horizontally polarized, the dielectric fluctuation depends on $\delta\varepsilon_{XY}(\mathbf{q},t)$ and $\delta\varepsilon_{YY}(\mathbf{q},t)$ component and scattering angle θ:

$$\delta\varepsilon_{HH}(\mathbf{q},t) = \delta\varepsilon_{XY}(\mathbf{q},t)\sin\theta + \delta\varepsilon_{YY}(\mathbf{q},t)\cos\theta. \qquad (2.14)$$

2.4 Detection technique for scattered light

Detection of scattered light mixing of scattered light with a coherent signal (optical mixing) followed by square law detection. There are two types of optical mixing experiments. One is called homodyne or self-beating detection and the other is called heterodyne detection. In the homodyne detection experiment, only the scattered light reaches the detector whereas in the heterodyne experiment a small portion of incident light is mixed with the scattered light. The autocorrelation functions of scattered light involved in the heterodyne and homodyne detections, denoted by $I_{if}^{(1)}(\mathbf{q},\ t)$ and $I_{if}^{(2)}(\mathbf{q},\ t)$, respectively are given by

$$I_{if}^{(1)}(\mathbf{q},\ t) = \left\langle \delta\varepsilon_{if}^{*}(\mathbf{q},0)\delta\varepsilon_{if}(\mathbf{q},t) \right\rangle \qquad (2.15)$$

$$I_{if}^{(2)}(q,t) = \left\langle \left| \delta\varepsilon_{if}^{*}(q,0) \right|^2 \left| \delta\varepsilon_{if}(q,t) \right|^2 \right\rangle \qquad (2.16)$$

The form of the dielectric tensor involved in scattering from spherical and cylindrical particles is considered.

2.5 Spherical molecule

The vector components of induced dipole moment, polarizability tensor $\boldsymbol{\alpha}$, and the electric field $\mathbf{E}$ of the incident light can be written as

$$\boldsymbol{\mu} = \begin{bmatrix} \mu_x \\ \mu_y \\ \mu_z \end{bmatrix} \tag{2.17a}$$

$$\boldsymbol{\alpha} = \begin{bmatrix} \alpha_{xx} & \alpha_{xy} & \alpha_{xz} \\ \alpha_{yx} & \alpha_{yy} & \alpha_{yz} \\ \alpha_{zx} & \alpha_{zy} & \alpha_{zz} \end{bmatrix} \tag{2.17b}$$

$$\mathbf{E} = \begin{bmatrix} E_x \\ E_y \\ E_z \end{bmatrix} \tag{2.17c}$$

The induced dipole moment can be expressed in component form as $\mu_\alpha = \alpha_{\alpha\beta} \, E_\beta$, where the indices α and β runs from 1 to 3 according to the correspondence 1=x, 2= y, 3=z in the Cartesian coordinate system. For an isotropic molecule, the polarizability $\boldsymbol{\alpha}$ can be expressed in terms of Kronecker delta symbol $\delta_{\alpha\beta}$ as $\alpha_{\alpha\beta} = \alpha \, \delta_{\alpha\beta}$, since the off-diagonal elements of the polarizability are zero and all diagonal elements have the same value α

The molecular polarizability α_{if} corresponding to the incident and scattered polarization directions $\mathbf{n_i}$ and $\mathbf{n_f}$ then can be written as

$$\alpha_{if} = (\mathbf{n_i}) \cdot \boldsymbol{\alpha} \cdot (\mathbf{n_f}) = (\mathbf{n_i})_\alpha \, \alpha_{\alpha\beta} \, (\mathbf{n_f})_\beta \,, \tag{2.18}$$

Now a fact has been used that for the case of spherical molecule $\alpha_{\alpha\beta} = \alpha \, \delta_{\alpha\beta}$. Then $\alpha_{if} = (\mathbf{n_i})_\alpha (\mathbf{n_f})_\alpha \alpha$ Using the summation equation

$$\alpha_{if}(1) = \sum_{\alpha=1}^{3} (\mathbf{n_i})_\alpha \cdot (\mathbf{n_f})_\alpha \cdot \alpha = \mathbf{n_i} \cdot \mathbf{n_f} \, \alpha \,. \tag{2.19}$$

13

Finally, the polarizability tensor for the whole sample becomes,

$$\alpha_{if}\left(\mathbf{q},t\right)=\mathbf{n_i}.\mathbf{n_f}\ \alpha\sum_{j=1}^{N}\exp\left(i\mathbf{q}.\mathbf{r}_j\left(t\right)\right)=\mathbf{n_i}.\mathbf{n_f}\ \alpha\ \Psi\left(\mathbf{q},t\right) \tag{2.20}$$

where $\Psi\left(\mathbf{q},\ t\right)=\sum_{j=1}^{N}\exp\left(i\mathbf{q}.\mathbf{r}_j\left(t\right)\right)$ and the summation is only over the particles which are under

illumination by the laser beam. If there are N (t) particles in the illuminated volume V at the time

t then

$$N\left(t\right)=\sum_{j=1}^{N}b_j\left(t\right) \tag{2.21}$$

where N is the total number of particle and $b_j\left(t\right)$ defines whether particles are inside the

illuminated volume V or not.

The total spectral density can be separated into two parts. The first part $I_{if}^{1}\left(t\right)$, referred to

as heterodyne spectral density, is proportional to $F_1\left(\mathbf{q},\ t\right)=\left\langle\Psi^{*}\left(\mathbf{q},0\right)\Psi\left(\mathbf{q},\ t\right)\right\rangle$ and the second

part $I_{if}^{2}\left(t\right)$, referred to as homodyne spectral density, is proportional to

$F_2\left(\mathbf{q},\ t\right)=\left\langle\left|\Psi^{*}\left(\mathbf{q},\ o\right)\right|^{2}\left|\Psi\left(\mathbf{q},\ t\right)\right|^{2}\right\rangle$. In the case of spherical molecules, depending on the

polarization directions of the incident and scattered light, the three different polarization

dependent spectral densities are

$$I_{VV}\left(\mathbf{q},t\right)=\alpha^{2}F_1\left(\mathbf{q},t\right) \tag{2.22}$$

$$I_{VH}\left(\mathbf{q},t\right)=I_{HV}\left(\mathbf{q},o\right)=0 \tag{2.23}$$

$$I_{HH}\left(\mathbf{q},t\right)=\cos^{2}\theta\ I_{VV}\left(\mathbf{q},t\right) \tag{2.24}$$

From $I_{VH}=0$, it is understood that the light scattered by a spherical molecule is not expected to

be depolarized and vertically polarized incident and scattered laser lights can be conveniently

14

chosen to characterize spherical molecules and the corresponding intensity is directly related to the heterodyne function

$$F_i(\mathbf{q},t) = \langle \Psi^*(\mathbf{q},o)\Psi(\mathbf{q},t) \rangle = < \sum_{j=1}^{N} b_j(0) \; b_j(t) \; \exp\left(i\mathbf{q}.[\mathbf{r}_j(t) - \mathbf{r}_j(0)]\right) > \qquad (2.25)$$

The maximum value of $\mathbf{r}_j(t) - \mathbf{r}_j(0)$ defines a characteristics length, L for translational motion. Initial position of a particle is $r_j(0)$ when it is inside the illuminated volume and after a L distance from that position, the particle leaves the illuminated volume. If the diffusion constant is D then the time scale of particle diffusion out of illuminated volume is $\tau = L^2 / D$. If the value of $r_j(t) - r_j(0)$ is close 1/q, the value of $\exp\left(i\mathbf{q}.[r_j(t) - r_j(0)]\right)$ deviates from 1. In that case the time scale is defined as is $\tau_q = \left(q^2 D\right)^{-1}$ and the ratio of these two time scale is $\dfrac{\tau}{\tau_q} = \left(qL\right)^2$. Now the quantity $b_j(0) \; b_j(t)$ changes over a much longer time scale than the value of $\exp\left(i\mathbf{q}.[r_j(t) - r_j(0)]\right)$. So, the approximation $b_j(0) \approx b_j(t)$ can be used and since the value of $b_j(0)$ is either 0 or 1 we can write $b_j(0) \; b_j(t) \approx b_j(0)$. Then the heterodyne function can be written as,

$$F_i(\mathbf{q},t) = \sum_{j=1}^{N} b_j(0) \; \exp\left(i\mathbf{q}.[r_j(t) - r_j(0)]\right) = \langle N \rangle F_s(\mathbf{q},t) \qquad (2.26)$$

where $F_s(q,t) = \left\langle \exp\left(iq.[r_j(t) - r_j(0)]\right) \right\rangle$, which is related to the probability distribution $G_s(\mathbf{R},t)$ for the particle to undergo a displacement R in time t. The relation is defined as

$$G_s(\mathbf{R},t) = \left\langle \delta\left(\mathbf{R} - \left[r_j(t) - r_j(0)\right]\right) \right\rangle \qquad (2.27)$$

and $\qquad F_s(\mathbf{q},t) = \int d^3\mathbf{R} e^{i\mathbf{q}.\mathbf{R}} \; G_s(\mathbf{R},t) \qquad (2.28)$

15

The probability distribution function $G_s(\mathbf{R}, t)$ is the solution of the diffusion equation,

$$\frac{\partial}{\partial t} G_s(\mathbf{R}, t) = D\nabla^2 G_s(\mathbf{R}, t).$$ (2.29)

The spatial Fourier transform of this equation is

$$\frac{\partial}{\partial t} F_s(\mathbf{q}, t) = -Dq^2 F_s(\mathbf{q}, t).$$ (2.30)

The solution of this equation is

$$F_s(\mathbf{q}, t) = \exp(-q^2 D) = \exp[-t/\tau_q]$$ (2.31)

According to the Einstein relation [3], the self-diffusion coefficient is $D = \dfrac{k_B T}{\xi}$, where

the friction is constant and according to the Strokes law, $\xi = 6\pi\eta a$ where η is the viscosity of the

solvent and a is the radius of the spherical molecule. So, the radius of the spherical molecule

can be determined from the heterodyne correlation function through the following equation,

$$F_1(q, t) = \langle N \rangle \exp(-q^2 D).$$ (2.32)

Similarly homodyne correlation function also can be used to determine the radius of spherical

molecule via the equation

$$F_2(q, t) = \langle N \rangle^2 + \langle N \rangle^2 \exp(-2q^2 Dt).$$ (2.33)

2.6 Nanorod model

Particles in a solution undergo two types of motion: translational and rotational. In the

case of a spherical particle both movements leave the particle orientation unchanged due to its

symmetrical shape. For a nanorod particle, on the other hand, these two movements can be

differentiated. The intensity of the scattered light depends on the orientation of the particle, so to

determine the size by autocorrelation of the scattered light intensity, both translational and

rotational diffusion motion must be taken into account. According to equation (2.10), the autocorrelation of the scattered light intensity is,

$$I_{if}^{\alpha}(\mathbf{q},\ t) = \sum_{j=1}^{N} < \alpha_{if}^{j}(0).\alpha_{if}^{j}(t).\exp i\mathbf{q}.\left[\mathbf{r}_{j}(t) - \mathbf{r}_{j}(0)\right] > \tag{2.34}$$

The term $\exp\left(i\mathbf{q}.\left[\mathbf{r}_{j}(t) - \mathbf{r}_{j}(0)\right]\right) = F_{s}(\mathbf{q},t)$ is related to the translational movement while the main autocorrelation of the polarizability tensor $\left\langle \alpha_{if}^{j}(0).\alpha_{if}^{j}(0)\right\rangle$ depends on both translational and rotational movement of the nano rod.

According to Fig (2.2) the incident light is propagating in the x-y plane, the polarization of the incident light $\mathbf{n}_{i}$ is in the z direction. The scattered light is omnidirectional. The scattered light along x axis is analyzed by observer. If the polarization of scattered light $\mathbf{n}_{f}$ is in z direction the autocorrelation is defined as $I_{VV}^{\alpha}(\mathbf{q},\ t)$ and if it's in y direction it's defined as $I_{VH}^{\alpha}(\mathbf{q},\ t)$. The autocorrelations in term of polarizability tensor are given below:

$$I_{VV}^{\alpha}(q,\ t) = \left\langle N\right\rangle \left\langle \alpha_{zz}^{j}(t).\alpha_{zz}^{j}(0)\right\rangle F_{s}(q,t) \tag{2.35}$$

$$I_{VH}^{\alpha}(q,\ t) = \left\langle N\right\rangle \left\langle \alpha_{yz}^{j}(t).\alpha_{yz}^{j}(0)\right\rangle F_{s}(q,t) \tag{2.36}$$
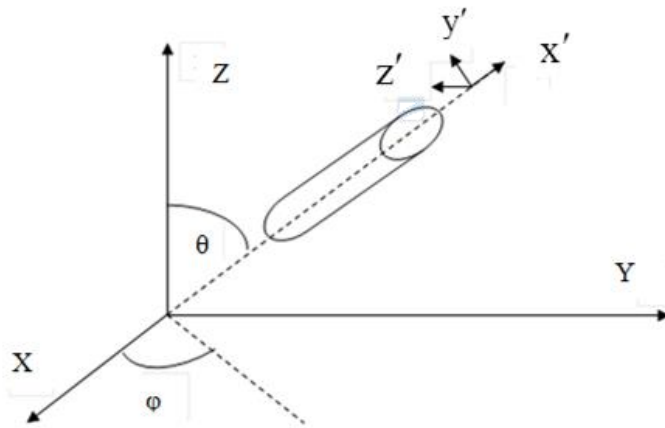
Fig(2.2): The laboratory and molecule-fixed coordinate system

17

The laboratory fixed coordinate system is defined as **XYZ** with corresponding unit vectors $\hat{x}$, $\hat{y}$ and $\hat{z}$ [Fig (2.2)]. On the other hand the molecule-fixed coordinate system is defined as **X'Y'Z'**. According to the orientation of the nanorod, X' makes angles ϕ and θ with X and Z respectively. **X'** is assumed along the principal axis of the nanorod. The molecule-fixed polarizability components are $\alpha_{\parallel}$ and $\alpha_{\perp}$, where $\alpha_{\parallel}$ refers to polarizability component parallel to **X'** axis and $\alpha_{\perp}$ refers to its component perpendicular to this axis. There are two axes perpendicular to **X'** axis: **Y'** and **Z'**. If the unit vectors along these two axis are defined as $\hat{y}$ and $\hat{z}$, $\hat{y}$ can be taken to lie in the **X'Z** plane and it makes an angle $(\frac{\pi}{2})$ with the **Z-axis**. The other unit vector $\hat{z}$ is perpendicular to the plane **X'Z,** and therefore to **Z.** So, **X'** changes with ϕ and **Y',Z'** changes with θ. This is how the molecular fixed coordinate system **X'Y'Z'** changes with the orientation of nanorod ϕ and θ.

The conversion of laboratory fixed unit vectors $\hat{z}$ and $\hat{y}$ of XYZ coordinate system into polar co-ordinate system and the matrix form of this polarizability is given below:

$$\hat{\mathbf{z}} = \begin{pmatrix} \cos\theta \\ \sin\theta \\ 0 \end{pmatrix} \quad (2.37a)$$

$$\hat{\mathbf{y}} = \begin{pmatrix} \sin\theta\sin\varphi \\ -\cos\theta\sin\varphi \\ -\cos\varphi \end{pmatrix} \quad (2.37b)$$

$$\boldsymbol{\alpha} = \begin{pmatrix} \alpha_{\parallel} & 0 & 0 \\ 0 & \alpha_{\perp} & 0 \\ 0 & 0 & \alpha_{\perp} \end{pmatrix} \quad (2.37c)$$

The laboratory fixed polarizability tensor becomes

$$\alpha_{zz} = \hat{\mathbf{z}} \cdot \mathbf{\alpha} \cdot \hat{\mathbf{z}} = \alpha_{\parallel} \cos^2\theta + \alpha_{\perp} \sin^2\theta \; ; \tag{2.38a}$$

$$\alpha_{yz} = \hat{\mathbf{y}} \cdot \mathbf{\alpha} \cdot \hat{\mathbf{z}} = \left(\alpha_{\parallel} - \alpha_{\perp}\right) \sin\theta \cos\theta \sin\varphi \tag{2.38b}$$

These components can be expressed in terms of spherical harmonics of order 2, $Y_{2,m}(\theta, \phi)$, as given below

$$\alpha_{zz} = \alpha + \left(\frac{16\pi}{45}\right)^{1/2} \beta \, Y_{2,0}(\theta, \varphi) \tag{2.39a}$$

$$\alpha_{yz} = i\left(\frac{2\pi}{15}\right)^{1/2} \beta\left[\, Y_{2,1}(\theta, \varphi) + Y_{2,-1}(\theta, \varphi)\right], \tag{2.39b}$$

where

$$Y_{2,0}(\theta, \varphi) = \sqrt{\frac{5}{16\pi}}\left(3\cos^2\theta - 1\right) \tag{2.40a}$$

$$Y_{2,m1}(\theta, \varphi) = m\sqrt{\frac{15}{8\pi}} \, \sin\theta \, \cos\theta \exp\left(\pm i\varphi\right) \tag{2.40b}$$

The two terms α and β are called isotropic and anisotropic part of the polarizability tensor respectively. The isotropic part $\alpha = \frac{1}{3}\left(\alpha_{\parallel} + 2\alpha_{\perp}\right)$ is the same in both the laboratory and molecule-fixed system because it does not depend on the orientation of the particle. The anisotropic part $\beta = \left(\alpha_{\parallel} - \alpha_{\perp}\right)$ is related to the orientation of the molecule.

In the molecule-fixed system the autocorrelation functions of scattered light can be expressed in terms of second order spherical harmonics as:

$$I_{VV}^{\alpha}(\mathbf{q}, t) = \langle N\rangle[\alpha^2\mathbf{F_s}(\mathbf{q}, t) + \left(\frac{16\pi}{45}\right)\beta^2 F_{2,0}^2(t)\mathbf{F_s}(\mathbf{q}, t) \tag{2.41}$$

$$I_{VH}^{\alpha}(\mathbf{q}, t) = \langle N\rangle\left(\frac{2\pi}{15}\right)\beta^2\left[F_{1,1}^{(2)}(t) + F_{1,-1}^{(2)}(t) + F_{-1,1}^{(2)}(t) + F_{-1,-1}^{(2)}(t)\right]\mathbf{F_s}(\mathbf{q}, t), \tag{2.42}$$

Where $F_{m,m'}^{(1)}(t) \equiv \left\langle Y_{lm'}^{*}(\theta(0)\varphi(0)) Y_{lm}(\theta(t)\varphi(t)) \right\rangle$ (2.43)

2.7 Analysis of rotational diffusion of a nano-rod

Each naorod particle goes through translational diffusion as well as rotational diffusion. In polar coordinate system the orientation of rod can be defined as (r,θ,ϕ). If r is assumed constant, the value of (θ, ϕ) changes due to rotational diffusion. A unit vector $\hat{u}$ can be defined along the principal axis of the cylindrical nanorod. If a sphere of unit is considered, then the orientation of the rod can be denoted by a point on the unit sphere [See Fig (2.3)]. The rod changes its position on the surface of the sphere due to rotational diffusion. According to Debye model the rod follows diffusion equation on the surface of the sphere:

$$\frac{\partial c}{\partial t} = D\nabla^2 c(r,t),$$ (2.44)

where r=1 and c(r, t) is the concentration of the rods at the surface of the sphere r=1.
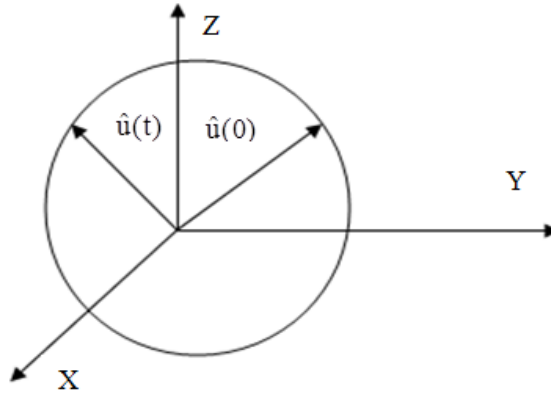
Fig (2.3): Rotational diffusion on surface of the unit vector radius sphere [1]

20

In the spherical coordinate system, the diffusion equation becomes,

$$\frac{\partial c(u,t)}{\partial t} = D_{rot} \frac{1}{\sin^2\theta}[\sin\theta\frac{\partial}{\partial\theta}(\sin\theta\frac{\partial}{\partial\theta}) + \frac{\partial^2}{\partial^2}]c(u,t) \tag{2.45}$$

where D_{rot} is the translational diffusion coefficient. Now, $\frac{1}{\sin^2\theta}[\sin\theta\frac{\partial}{\partial\theta}(\sin\theta\frac{\partial}{\partial\theta}) + \frac{\partial^2}{\partial^2}]$ can be

defined as the operator, $-\hat{L}^2$. So, the diffusion equation becomes

$$\frac{\partial c(u,t)}{\partial t} = -D_{rot} \cdot \hat{L}^2 c(u,t) \tag{2.46}$$

The solution of this diffusion coefficient in terms of spherical harmonics is given below:

$$c(u,t) = \exp\left(-tD_{rot} \cdot \hat{L}^2\right) c(u,0) \tag{2.47}$$

where

$$c(u,0) = \delta(u-u_o) = \sum_{lm} Y_{lm}(u_o) Y_{lm}^*(u) \tag{2.48}$$

and

$$\delta(u-u_o) = \sum_{l=0}^{\infty}\sum_{lm=-1}^{+1} Y_{lm}(u_o) Y_{lm}^*(u) \tag{2.49}$$

Now, since $-\hat{L}^2 Y_{lm}(u) = 1(1+1) Y_{lm}(u)$ the solution becomes,

$$c(u,t) = \sum_{lm}\exp\left[-1(1+1)D_{rot}t\right] Y_{lm}(u_o) Y_{lm}^*(u) \tag{2.50}$$

The concentration c (u, t) can be treated as the transition probability, $K_s(u,t\,|\,u_o,0)$ of the

rod, i.e., the probability of the rod to transit to a point u at t time given that it was at u_o at time

t=0. If t→∞, the transition probability becomes 1/4π. This means after a long time, the rod will

be uniformly distributed on the whole surface. According to the transition probability, the term

$F_{m',m}^{(1)}(t)$ in equation (2.32) becomes

$$F_{m',m}^{(1)}(t) = \frac{1}{4\pi}\exp\left(-1(1+1)D_{rot}t\right)\int d^2u Y_{l'm'}\left(\mathbf{u}(0)\right) Y_{lm}^*\left(\mathbf{u}(t)\right) \tag{2.51}$$

where the correlation function become 0 unless $1=1'$ and $m=m'$. Finally equation (2.30) and (2.31) becomes,

$$I_{VV}^{\alpha}(\mathbf{q},\, t) = \langle N \rangle \{\alpha^2 + \left(\frac{4}{45}\right)\beta^2 \exp(-6D_{rot}t)\} \exp(-q^2 D_{tr} t) \tag{2.52}$$

$$I_{VH}^{\alpha}(\mathbf{q},\, t) = \langle N \rangle \left(\frac{1}{15}\right)\beta^2 \exp\left(-6D_{rot}t\right)\exp(-q^2 D_{tr} t) \tag{2.53}$$

The diffusion coefficients can be expressed in terms of translational relaxation rate ($\Gamma_{tr} = q^2 D_{tr}$) and rotational relaxation rate ($\Gamma_{rot} = -6D_{rot}$). The autocorrelation of the scattered light then becomes,

$$I_{VV}^{\alpha}(\mathbf{q},\, t) = A\exp\left(-\Gamma_{tr}t\right) + B\exp[-(\Gamma_{tr} + \Gamma_{rot})t] \tag{2.54}$$

where $A = \langle N \rangle \alpha^2$ and $B = \langle N \rangle \left(\frac{4}{45}\right)\beta^2$

$$I_{VH}^{\alpha}(\mathbf{q},\, t) = C\exp\left[-(\Gamma_{tr} + \Gamma_{rot})t\right], \tag{2.55}$$

where $C = \langle N \rangle \left(\frac{1}{15}\right)\beta^2$.

The relation between the translational diffusion coefficient and length of the nano rod is

$$D_{tr} = \frac{k_B T}{3\pi\eta L}F(AR) \tag{2.56}$$

where F(AR) is the model dependent aspect ratio function. The equation for this function is [4] :

$$F(AR) = \ln(AR) + 0.312 + \frac{0.565}{AR} - \frac{0.1}{AR^2} \tag{2.57}$$

Another relation for length of the nano rod and rotational diffusion coefficient is

$$D_{rot} = \frac{3k_B T}{\pi\eta L^3}G(AR) \tag{2.58}$$

where G (AR) is another model dependent function of aspect ratio given by [4]:

22

$$G(AR) = \ln(AR) - 0.662 + \frac{0.917}{AR} - \frac{0.05}{AR^2} \qquad (2.59)$$

Another term is defined as H(AR) which is a constant and can be obtained from the ratio of G(AR) and F(AR). In Fig (2.4) the F(AR), G(AR) and H(AR) is plotted where the value of H(AR) is approximately 0.5. In practice, two relaxation rates are obtained from the autocorrelation function of the scattered light; the translational relaxation rate, Γ_{tr} and the mixed relaxation rate, $\Gamma_{mix} = (\Gamma_{tr} + \Gamma_{rot})$. By combining these two equations, the length of nano rod can be expressed in terms of translational and rotational relaxation rate,

$$L = q^{-1} \sqrt{54 \left(\frac{\Gamma_{rot}}{\Gamma_{tr}} \right)^{-1} H(AR)} \ , \qquad (2.60)$$

To determine the aspect ratio of the nanorod, the length, determined from equation 2.59 is used in equation 2.55 or 2.57. Then the solution of any of these equations will be the aspect ratio of the nanorod.
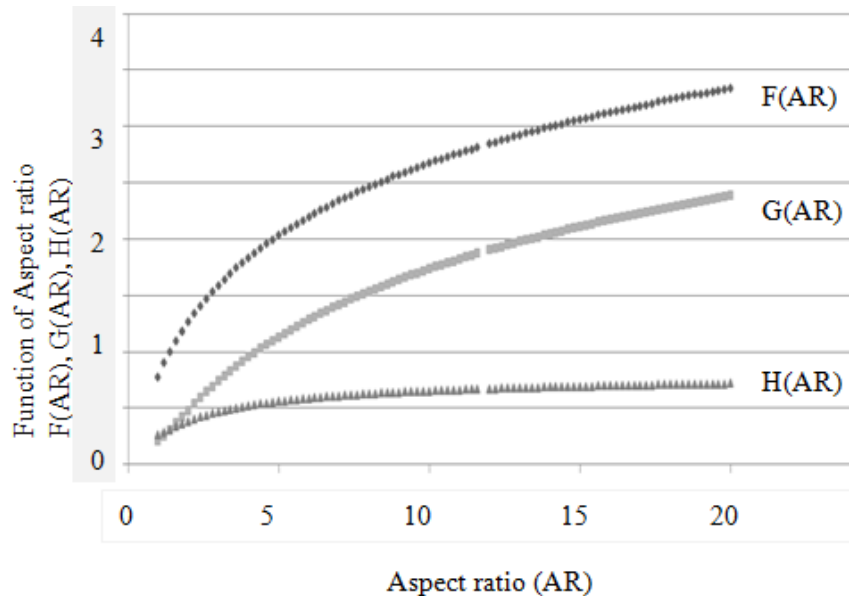
Fig (2.4): Function of aspect ratio F (AR), G (AR), H (AR) versus the aspect ratio (AR) [4]

23

Chapter 3

Experimental setup

   To perform dynamic light scattering experiments, a goniometer (BI-200SM) with a scattering cell, a photoelectric detector and a digital autocorrelator equipped with light scattering software were used. This set up can be used to do the average time integrated intensity measurement to calculate the molecular size, radius of gyration and second virial coefficient of any polymer solution. It is also used to carry out dynamical light scattering (DLS) experiment to calculate the diffusion coefficient and particle size distribution. In addition to the hardware and software mentioned above a laser light source and associated optics (polarizers, lenses and mirrors) for beam alignment were also needed. An outline of the experimental set up is shown in Fig. (3.1). The principal components of the apparatus is now decribed.

The hardware of this experiment is divided into five parts [see Fig (3.1)]:

- Laser light source

- Beam Steering Optics

- Goniometer

- Photo-detector: Photo multiplier tube (PMT)

- Temperature Controller

3.1 Laser light source

   A He: Ne laser operating at 632.8 nm was used to supply the incident light for this experiment. A highly reflective plane mirror and a concave mirror made the Fabry-Perot cavity of this laser. The output came from the concave mirror. He: Ne mixture used as its gain medium which was excited by a high voltage electric discharge. The output power of the laser light was 25 mW. The output beam from the laser had a Gaussian beam profile with a beam spot diameter of approximately 2 mm.

24

3.2 Beam steering optics

Two sets of optical elements were used for this experiment. The first set was to make the incident laser light vertically polarized and to guide it to the sample holder. The other set of optical elements used to collect vertically or horizontally polarized scattering light and guide it to the detector (a photo-multiplier tube).

Pre scattering optical system: A set of steering plane mirrors guided the laser beam to a lens of focal length 10 cm mounted on the goniometer. The lens focused the beam, through entrance aperture, onto the sample holder located at the center of rotation of the goniometer.

Post scattering optical system: A second 10 cm focal length lens in front of the PMT collected and focused the scattered light and guided it to the photomultiplier aperture. The lateral position of this lens adjusted by two screws.

Slit adjustment: The amount of scattered light that enters the photomultiplier controlled by adjusting the aperture in front of the colleting lens. The apparatus position was changed horizontally by two screws provided for this purpose.

Pinhole wheel: The pinhole was to change the amount of scattered light that enter into the photomultiplier. The pinhole wheel can be change to 100, 200 and 400micron for QELS measurement and 1mm, 2mm and 3mm for classical measurement.

Filter wheel: There was also a filter wheel to select scattered light of desired wavelength to prevent stray and background light from other sources than the laser from reaching the photomultiplier tube. This set up allowed to do the experiment using light with wavelengths 633nm, 514 nm and 488nm.

3.3 Goniometer

Precision machined base: This was the bottom part of the whole set up. The turntable, rigid rotating arm, center of rotation adjustment table and the cell are all attached to the base, which was fixed to the optical table.

Turntable: This table was mounted on the precision machined base. There was a circular scale on the outside of this table which was used for all angle measurement in this experiment.

Detector rail: This rail was contained all after-scattering detector optics and photomultiplier tube assembly. Its angle relative to the forward scattering direction was changed by rotating the detector rail. In this experiment this angle was fixed at 90° to the forward scattering direction.

Center of rotation adjustment: The position of the sample cell was adjusted to coincide with the center of rotation of the table to optimize scattering signal.
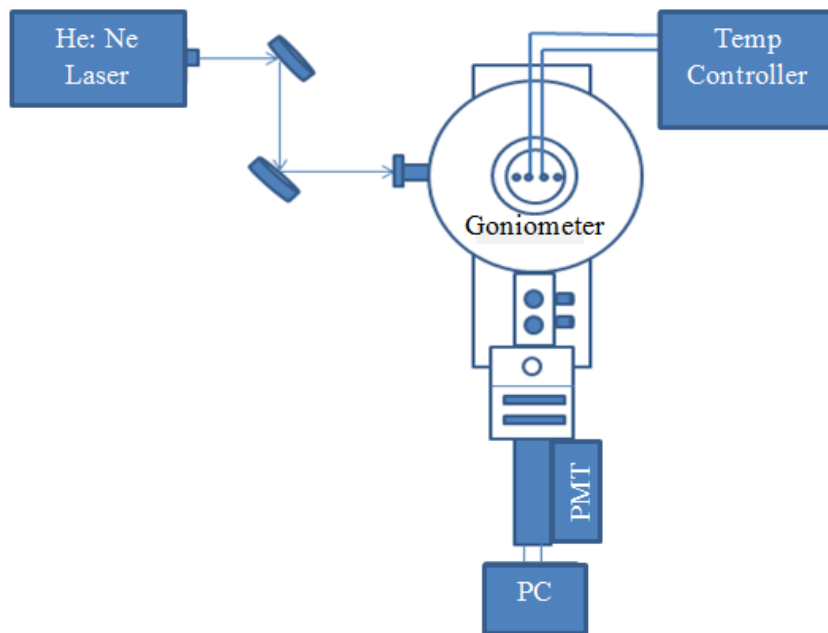
Fig (3.1): Diagram of set up (Top view)

The sample cell holder assembly was a metal pot which was insulated and anodized. This cell contained a special glass VAT with approximately 100 ml of an index matched liquid usually Decalin. It also served as a bath to control the temperature of the sample. The VAT and the center of rotation were concentric. The sample holder was submerged from the top of the sample cell assembly. There were also two other pair of hole on top of it for allowing circulation tubes for temperature control fluid and filtration of decalin. During the alignment time a target pattern was used to check shape of the laser beam exiting the scattering region. The target pattern was located on the wall after the sample cell assembly. During the experiment, the exit laser beam was blocked with a beam stop to reduce scattering and for eye safely.

3.4 Photomultiplier tube

A photomultiplier operated in the single-photon counting mode, along with a high voltage power supply was the scattered light detector of the set up to count and correlate photons. This photo multiplier converted photons into corresponding photoelectric pulses which were sent two a digital correlator on a PC circuit board.

3.5 Temperature controller

The external temperature controller was used to change the temperature of the sample solution by changing the temperature of decalin. Ethylene glycol was used with DI water in 1:1 ratio. The temperature of the sample controlled from 5 C to 80 C by circulating Ethylene glycol-water mixture.

Chapter 4

Data Analysis

4.1 Measuring the correlation function

The multiplication of two signals with one signal time delayed by and interval τ relative to the other is called correlation of the two signals or the cross correlation function. If there are two signals called A(t) and B(t), the in general correlation $C(\tau)$ with time delay τ is given by

$$C(\tau) = \lim_{T \to \infty} \frac{1}{T} \int_{t_o}^{t_o + T} A(t).B(t - \tau).dt \qquad (4.1)$$

where t_o is the initial time and T is the integration time. It characterizes the relation between two signals at different time.

The correlation between a signal with its time-delayed version is called the auto-correlation function. If the signal is A (t) and the time delay is τ, the auto correlation function $R(\tau)$ is defined as

$$R(\tau) = \lim_{T \to \infty} \frac{1}{T} \int_{t_o}^{t_o + T} A(t).A(t - \tau).dt . \qquad (4.2)$$

The variation of correlation of a signal at different time can be observed by auto correlation function (ACF). The figure below shows the typical form of a correlation function as a function of time delay τ. In general, it decays with time delay and approaches a value corresponding to a value corresponding to the product of the averages of the two signals as the relative delay increases.

Correlations are maximum for short delays but are reduced as time delay increases. At $\tau = 0$ the ACF becomes $<A^2>$ and when $\tau = \infty$, ACF becomes $\langle A \rangle^2$. Thus the ACF decays

from $<A^2>$ to $\langle A \rangle^2$ as a function of the decay time τ , which is the characteristics property of the molecule to be measured.
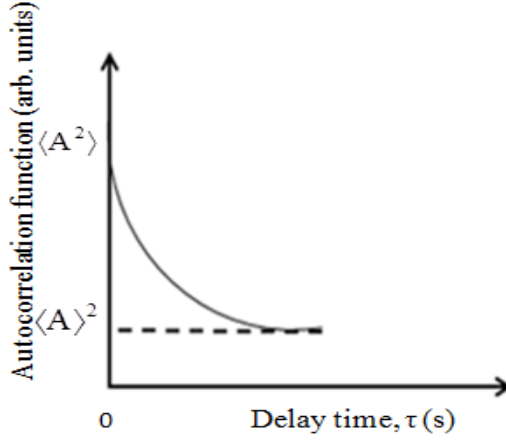
Fig(4.1): Autocorrelation function [2]

After multiplication of two signals, integration over T time is done to get the cross correlation or auto correlation function. The delay time is an integer multiple of sampling time $\Delta\tau$. In a linearly spaced correlator, the last delay time is $\tau_f = N\Delta\tau$. If n_i is the number of pulses during the sampling time $\Delta\tau$ centered at time t, and n_{i-j} is the number of pulses during sampling time $\Delta\tau$ centered at $t - \tau_j$, where τ_j is the jth delay time, then the Approximate Auto Correlation Function (ACF) is

$$R\left(\tau_j\right) = \lim_{N \to \infty} \frac{1}{N} \sum_{i=1}^{N} n_i . n_{i-j}, \qquad j = 1, 2, 3....M \qquad (4.3)$$

where the number of correlator channels is M. The number of pulses, n in a sampling time is average count rate multiplied by the sampling time.

The second order intensity autocorrelation function of scattered is an unnormalized auto correlation function, which is denoted by $G^{(2)}\left(\tau\right)$, where τ is delay time. The first order electric

29

field autocorrelation function is defined as $g^{(1)}(\tau)$. The relation between intensity and electric field autocorrelation function is called Siegert relationship which is given below

$$G^{(2)}(\tau) = B(1 + f^2 |g^{(1)}(\tau)|^2), \tag{4.4}$$

where B is based line, which is determined by the value of the correlation function at infinite time delay and is proportional to the square of the average intensity. The amplitude f is the zero delay correlation function intercept to baseline ratio and it depends on the laser beam and detector optics. This Siegert relationship is not applicable to non-ergodic or non-Gaussian fluctuations. The electric field auto correlation function for self-beating or homodyne system is given in equation 4.5 where the relaxation rate $\Gamma = \dfrac{1}{\tau_r}$ where τ_r is the decay time.

$$|g^{(1)}(\tau)| = \exp(-\Gamma \tau) \tag{4.5}$$

For a dilute system if the decay is purely translational (i.e. spherical particle), the decay rate, $\Gamma = D_T.q^2$, where D_T is translational diffusion coefficient and q is scattering wave vector. For a dilute system, D_T is given by the Stokes-Einstein relation,

$$D_T = D_o = \frac{\kappa_B T}{3\pi\eta_l d_H}, \tag{4.6}$$

where k_B is the Boltzmann constant, T is the absolute temperature, eta is the viscosity of the fluid and d_H is the Hydrodynamic diameter of the particle to be measured.

4.2 Model fitting

Depending on the shape, size and uniformity of these particle attributes in the scattering medium, different types of data fittings are needed. These include, Cumulant, Williams-Watts,

double exponential fits etc. In this thesis the spherical and nanorod particle sizes were studied and cumulant and double exponential fitting were used to analyze the data.

4.2.1 Cumulant fit

In cumulant data fitting, the mean, variance, and kurtosis of the variable of interest can be measured by determining its moments. It is assumed that the variable of interest is a random variable characterized by a distribution. The moments of this distribution quantify its shape. If X is random number and f (x) is the probability density such that f (x) dx is probability that variable X has a value between x and x+dx, then the rth moment of X is defined as

$$\mu_r = E\left(X^r\right) = \int_{-\infty}^{+\infty} x^r f\left(x\right) dx \tag{4.7}$$

where r=0, 1, 2, … is the order of the moment and E (X^r) represents the average value of the X^r. All of these moments can be defined by a moment generating function, $M(\xi)$ with parameter ξ. The Taylor expansion of the moment generating function is given below,

$$M(\xi) = E\left(e^{\xi X}\right) = E\left(1 + \xi X + \xi^2 \frac{X^2}{2!} + \ldots\right) = \sum_{r=0}^{\infty} \mu_r \frac{\xi^r}{r!} \tag{4.8}$$

The logarithm of the moment generating function gives the cumulant generating function. If a Taylor series expansion of the cumulant generating function in powers of ξ is made, it gives

$$K(\xi) = \log M(\xi) = \sum_{r=1} K_r \frac{\xi^r}{r!} \tag{4.9}$$

where the coefficient of ξ^r is the rth cumulant K_r. The cumulants can be expressed in terms of moments. The first cumulant $K_0 = 0$ because the first moment $\mu_0 = 1$. The second cumulant K_1 is the mean of moment μ_1, the third cumulant K_2 is the variance $\mu_2 - \mu_1^2$ etc.

In the autocorrelation function of the scattered light, the relaxation rates have a distribution because, strictly speaking, all the particles do not have the same size. Assuming that the relaxation rates are distributed according to the distribution function $G(\Gamma)$. According to cumulant data fit, the radius of gyration, hydrodynamic radius, and effective diameter, polydispersity, skew, kurtosis etc of a molecule can be determined. In terms of $G^{(2)}(\Gamma)$, the auto correlation can be expressed as

$$g^{(1)}(\tau) = \int_0^\infty G^{(2)}(\Gamma) \exp(-\Gamma.\tau).d\Gamma, \tag{4.10}$$

where,
$$\int_0^\infty G^{(2)}(\Gamma).d\Gamma = 1 \tag{4.11}$$

Then a Taylor series expansion of the autocorrelation about the mean $\bar{L}$ of the relaxation rate gives
$$g^{(1)}(\tau) = \exp(-\bar{L}\tau).\left[1 + \frac{\mu_2}{2!}.\tau^2 + \frac{\mu_3}{3!}.\tau^3 + \frac{\mu_4}{4!}.\tau^4 + ...\right] \tag{4.12}$$

The first moment of the series is defined as $\bar{L} = \int_0^\infty \Gamma.G^{(2)}(\Gamma)d\Gamma$ and the nth moment is defined as

$$\mu_n = \int_0^\infty (\Gamma - \bar{L}).G^{(2)}(\Gamma)d\Gamma \tag{4.13}$$

Multiplying both sides of Eq. (4.13) by f, taking the natural logarithm of both sides and expanding the autocorrelation function in powers of τ, we get

$$\ln\left[f\left|g^{(1)}(\tau)\right|\right]=\ln(f)-\bar{L}\tau+\frac{\mu_2}{2!}.\tau^2-\frac{\mu_3}{3!}.\tau^3+\frac{\mu_4-3\mu_2^2}{4!}.\tau^4+\dots \qquad (4.14)$$

The coefficients of τ^n are the cumulants of relaxation rate and different characteristics of material can be found from these cumulant terms.

The radius of the spherical particle can be determined by the first moment because the first moment, $\bar{L}=\bar{D}_r.\dot{q}$. In this condition the first moment depends on particle size and molecular weight. So, the first moment directly gives effective diameter, d_H through diffusion coefficient.

The effective diameter also can be measured from higher order cumulants since all cumulants are actually function of decay rate $\bar{L}$. Moreover the second moment μ_2 gives the polydispersity $\mu_2/\bar{L}$ which is the width of the decay rate. The third moment, μ_3 gives the skewness $(\mu_3/\mu_2^{\frac{3}{2}})$ of the Gaussian distribution. The forth moment μ_4 gives the so-called kurtosis (μ_4/μ_2^2) or the peakedness of the Gaussian distribution. In the software, depending on the number of moments desired, there are four different types of cumulant fits; linear, quadratic, cubic and quartic.

4.2.2 Double exponential fit

This is a fit of the broad and nonlinear auto correlation function with a double exponential for the auto correlation function as

$$g^{(1)}(\tau)=G(\Gamma_1).\exp(-\Gamma_1.\tau)+G(\Gamma_1).\exp(-\Gamma_2.\tau) \qquad (4.15)$$

where $G(\Gamma_i)$ is the relative intensity contributed scatterers with decay rate Γ_i.

Figure (4.2) shows a graphical representation of this correlation function. The vertical bars represent the weight of two exponential decays terms, the height (y) of the bar being the relative intensity and the x value of the bar the relaxation or decay rate (Γ_i) of the exponential.
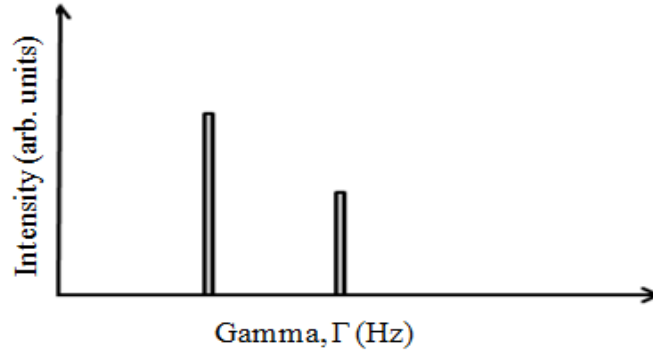
Fig (4.2): Relaxation rate, Γ versus scattered light intensity.

In case of nano-rod particles, if the depolarized scattered light is used (v-h measurement), only one relaxation rate will be available and according to the equation 2.54 this is mixed relaxation rate (mixed of translational and rotational relaxation rate) which can be extracted by one exponential fitting. On the other hand, if the scattered light is vertically polarized (v-v measurement) there should be a minimum of two relaxation rates and according to the equation 2.53, one of these relaxation rates is mixed relaxation rate and another one is translational relaxation rate. So, the mixed relaxation rate can be measure in two different ways. The rotational rate is usually much higher than the translational rate so the mixed relaxation rate is much higher than the translational rate. So it's simple to distinguish between these two decay rates. The auto correlation function for depolarized scattering light signal from nanorod sample is given by

$$g(\tau) = G(\Gamma_1).\exp(-\Gamma_{tr}.\tau) \qquad (4.16)$$

34

The auto correlation function for polarized scattering light signal from nanorod sample is given by

$$g(\tau) = G(\Gamma_{tr}).\exp(-\Gamma_{tr}.\tau) + G(\Gamma_{mix}).\exp(-\Gamma_{mix}.\tau), \qquad (4.17)$$

where $\Gamma_{mix} = \Gamma_{tr} + \Gamma_{rot}$

According to the theory, the length of the nanorod [4],

$$L = q^{-1}\sqrt{\frac{54\Gamma_{tr}H(AR)}{\Gamma_{rot}}} \qquad (4.18)$$

Where q is the wave vector, Γ_{tr} is the translational relaxation rate, Γ_{rot} is the rotational relaxation rate and H(AR) is a constant which can be obtained from the model dependent translational and rotational functions F(AR) and G(AR) respectively. The aspect ratio can be obtained according to the equation 2.55, $F(AR) = \dfrac{3\pi\eta\Gamma_{tr}L}{k_BTq^2}$. So, from double exponential fitting the length and aspect ratio of nanorod can be obtained.

Chapter 5

Experimental results

In these experiments the dynamic light scattering technique, described in previous chapters was used to determin the length L and aspect ratio AR (or the diameter) of three nano-rod samples. The radius of a spherical particle was determined for calibration. The temperature dependence of the diffusion coefficient of the spherical particle was also a part of the calibration. A description of the procedure for cleaning the sample holder, calibration and the final experimental results is given below.

5.1 Calibration:

The cleaning and filtering procedure was essential in this experiment. As the particles to be measured were in nanometer range, all solutions needed to be filtered by 20 nm syringe filter. The cleaning of test tube was done in five steps. At first, the test tube was submerged for 10 minutes in a 3:1 sulfuric acid and hydrogen per oxide mixture. After 10 minutes, the test tube was rinsed, one after another, by de-ionized (DI) water, acetone, DI water, isopropyl alcohol and DI water. Finally the test tube was dried in an air drier. After cleaning the sample holder, the DLS experimental result or the auto correlation function with the sample holder containing only DI water was a flat curve consisting of random points since there were no particles to scatter the incident light. The count rate was also very low which was below 1Kcps. The auto correlation function of the experiment for DI water is given in Fig (5.1).
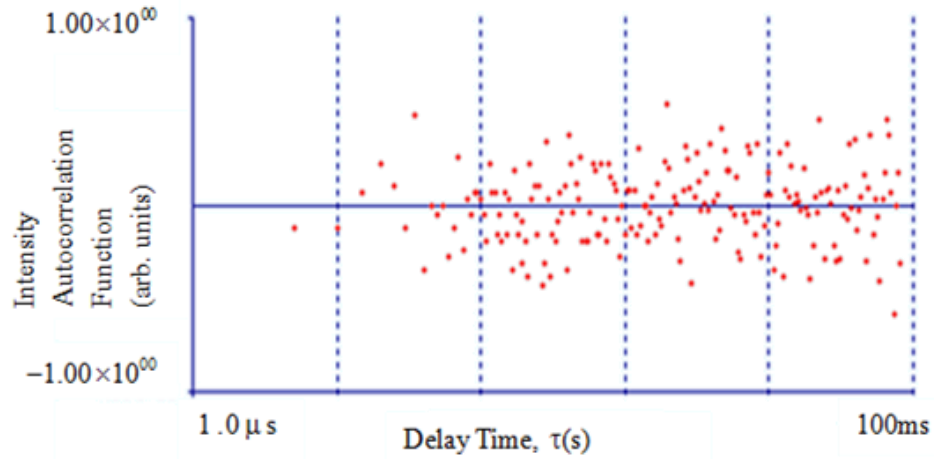
Fig (5.1): Auto correlation function of the experiment when the solution is only DI water.

After cleaning, it was necessary to know the concentration of nano-particle in the solution, as the count rate was proportional to the concentration and it should not exceed 100Kcps. The formula of count rate is given below:

$$CR = \frac{NV_s \Phi \Omega \sigma}{4\pi},$$ (5.1)

where N is the concentration of particle, V_s is illuminated volume of the sample, Φ is photon flux, Ω is solid angle subtended by the detector on the sample volume and σ is the scattering probability. The illuminated volume was determined by the laser light beam width w_o and the test tube width a as the formula for illuminated volume is $V_s = a \times \pi w_o^2$. The solid angle Ω was also determined by the detector aperture width and the distance of the aperture from the sample holder. In Fig (5.2) count rate of the experiment of DI water as a function of times is shown.

37
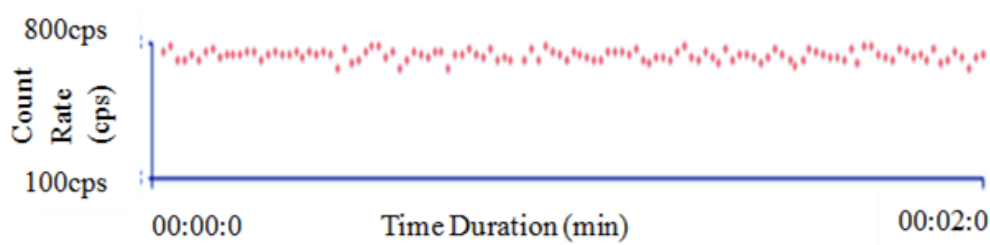
Fig (5.2): Count rate of the experiment when the solution is only DI water

To ensure that the DLS system was working properly, polystyrene nanospheres dispersed in water were used as scatterers for calibration. The manufacture provided diameter of these particles was 93 nm+/-5nm. The result of nanosphere diameter determined by cumulant data analysis is given in Table 5.1. The radius of the sphere is determined as 100 nm which was around 8% larger to the manufacturer's value.

	Relaxation rate Γ (s^{-1} or Hz)	Diffusion coefficient D_o (cm^2s^{-1})	Hydrodynamic diameter d_H (nm)
Linear	1.4×10^3	4.0×10^8	100
Quadratic	1.5×10^3	4.2×10^8	96
Cubic	1.4×10^3	4.0×10^8	101
Quartic	1.4×10^3	3.9×10^8	103

Table 5.1 The result of nano sphere particle

Another test to check the proper working of the DLS system was to study the temperature dependence of the diffusion constant. According to Equation 4.4, the hydrodynamic diameter of the particle is d_H .

$$D_o = \frac{\kappa_B T}{3\pi\eta_l d_H}, \qquad\qquad (5.2)$$

So, for a stable particle the diffusion coefficient is proportional to the temperature T and

the value of $\dfrac{\kappa_B}{3\pi\eta_l d_H}$ is constant. So, Equation 5.2 is an equation for straight line as a function of

temperature T. The graph of Diffusion coefficient, D_o versus Temperature was a straight line as

shown in Fig (5.3). The measurement of diameter and the temperature dependence of the

Polystyrene nanosphere confirmed that the DLS system was functioning properly and was ready

to be used for the measurements on nanorods.
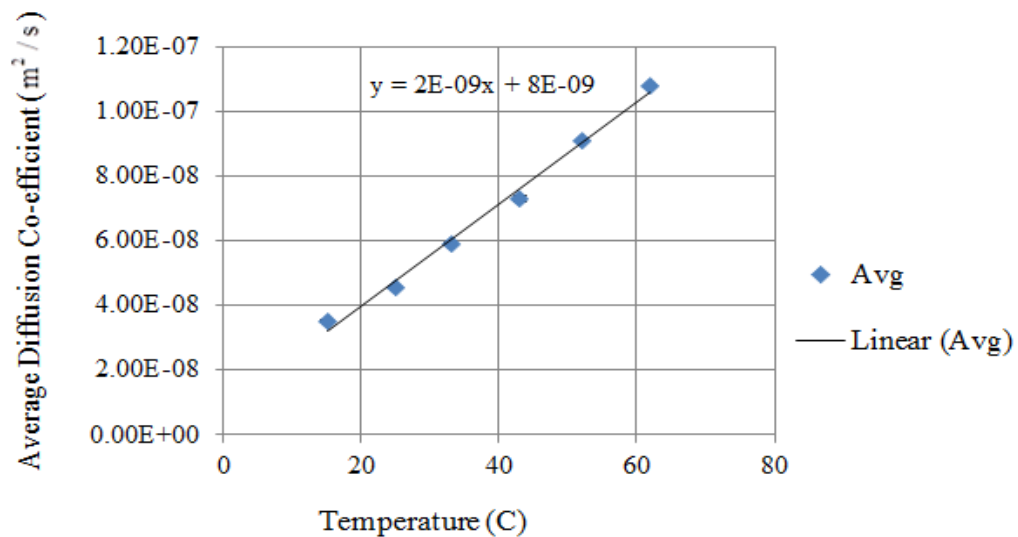
Fig (5.3): The diffusion Coefficient m^2/s versus Temperature(C) Graph

5.2 Experiment

In the final experiment, three different nanorods samples were measured. Those nano-

rods were labeled as 001, RPD700D and RPD235AD. Both polarized (VV) and depolarized

(VH) light experiments were carried out for the three samples and each experiment was repeated

twenty five times except in the first case due to insufficient sample amount. In the polarized experiment, both incident and scattered lights were vertically polarized and in depolarized experiment, the incident light was vertically polarized but the scattered light was horizontally polarized.

The double exponential fitting was used for polarized (VV) light experiment and from the relaxation rate verses scattered light intensity graph, the translational and mixed relaxation rates were determined. The rotational diffusion relaxation rate was determined from the subtract of the translational and mixed relaxation rates. The length of the nano rod was then determined by using equation 4.18. Later the aspect ratio and the diameter of the nano rod were also calculated. The detailed results for each sample are summarized below:

5.2.1 Sample 001:

The material of these nano rods was $AuCu_3$. [7] These nanorods were dispersed in Toluene. The manufacturer provided TEM image of sample 001 is shown in Fig (5.4) where the average length of the nanorod was 25nm and the average diameter was 8nm.The concentration of nano rod was 7.8×10^{13} particle/ml. Special care was needed to avoid the evaporation of Toluene. The published viscosity of Toluene was 0.558cP, and the published Refractive Index was 1.496.
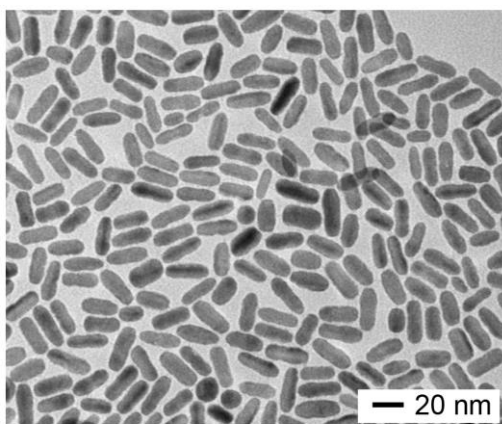
Fig (5.4): TEM image of sample 001[7]

Since the scattering angle of the experiment was 90 degree, the scattering wave vector was

$$q = \frac{4\pi\eta}{\lambda}\sin\left(\frac{\theta}{2}\right) = \frac{4\times3.14\times1.496}{633nm}\sin\left(\frac{90}{2}\right) = 0.021/nm \qquad (5.3)$$

The first experiment was a vertically polarized scattered light (VV) experiment. The auto correlation function and the relaxation rate versus scattered light intensity graph are shown in Fig (5.5)
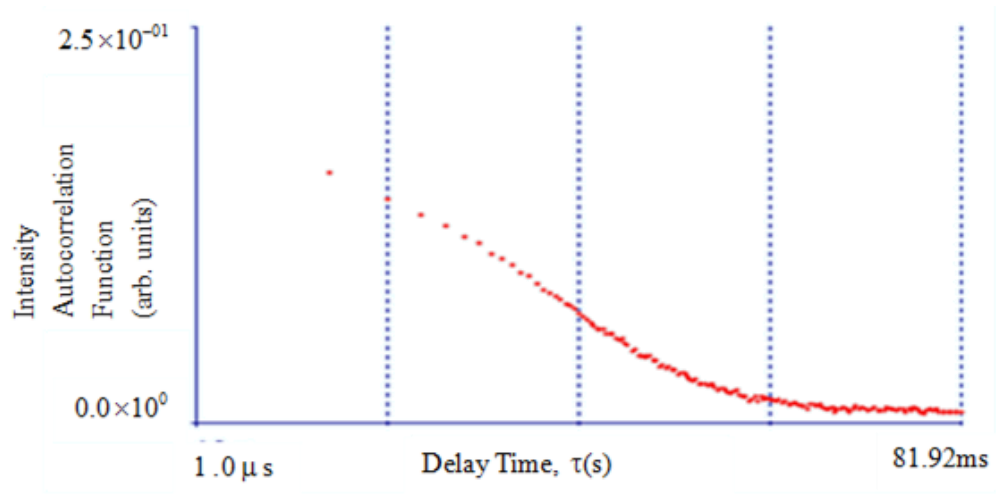
Fig (5.5) Autocorrelation function for polarized scattered light (VV) experiment for sample 001

The relaxation rate vs scattered light intensity graph for sample 001 is shown in Fig (5.6). The translational and mixed relaxation rate was found from this figure.
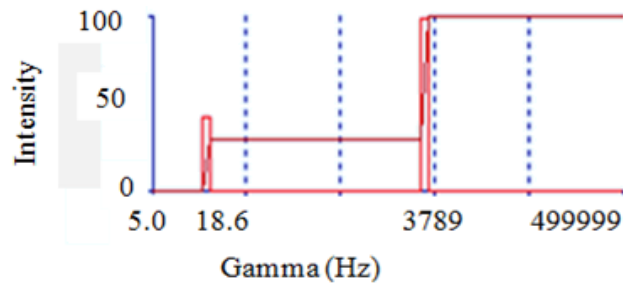
Fig (5.6): Relaxation rate intensity (weight) versus relaxation rate graph for sample 001.

The second experiment on the same nanorod sample was depolarized scattered light (VH) measurement. The auto correlation function is shown in Fig (5.7). No meaningful relaxation rate could be extracted from the data for this nanorod sample.
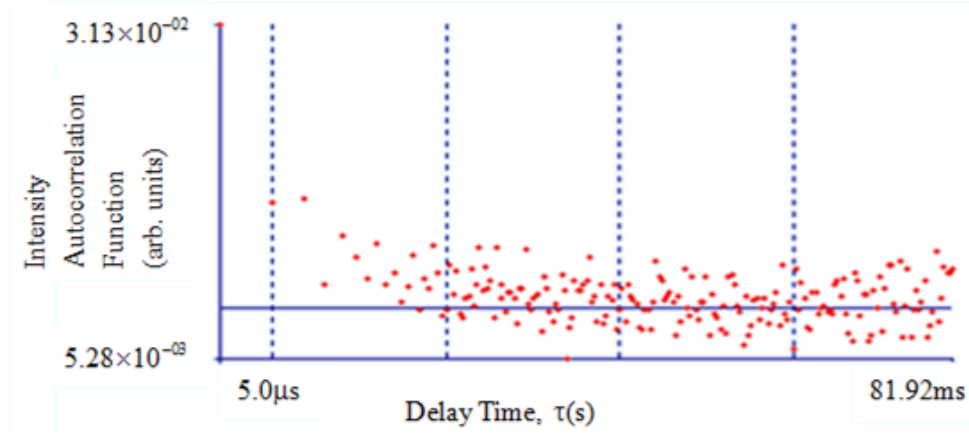
Fig (5.7): The autocorrelation function for depolarized experiment for sample 001.

The results for this sample are shown in Table 5.1. First, the length is determined from the translational and rotational relaxation rates. Then the aspect ratio and diameter are calculated.

Run	Translational relaxation rate Γ_{tr} (Hz)	Mixed relaxation rate Γ_{mix} (Hz) (Polarized)	Mixed relaxation rate Γ_{mix} (Hz) (Depolarized)	Rotational relaxation rate Γ_{rot} (Hz) (Polarized)	Length L (nm)	Aspect ratio	Diameter d (nm)
1	16	3645	-	3629	20	1.97	10
2	19	3789	-	3770	21	1.97	11
3	6	3150	-	3144	13	1.97	7

Table5.2: Result of sample 001

5.2.2 Sample RPD700D:

This was a bare Gold (Au) nanorod sample with CTAB (Cetyl trimethyl ammonium bromide) coating to keep the nanorod separate from each other. It was diluted in DI water. The concentration of nanorods was 8.11×10^{11} particle /ml. The published Refractive Index

of DI water was 1.33. Since the scattering angle of the experiment was 90 degree, the viscosity of DI water was 1.15cP , then the scattering wave vector was calculated to be 0.018/nm. The TEM image of this sample was shown in Fig (5.8) which was taken in laboratory. According to this image the distribution of length was 23 ± 7nm and distribution of diameter was 10 ± 2nm.
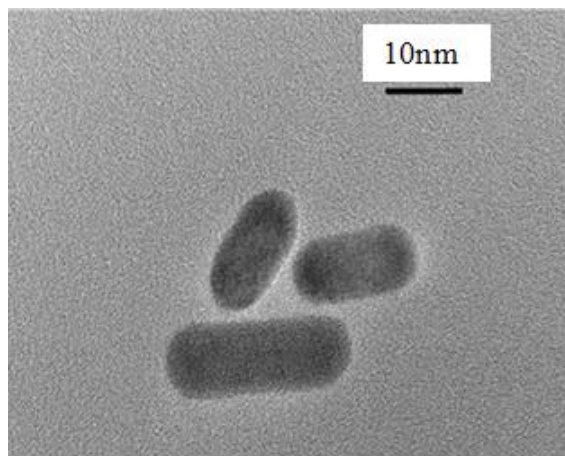
Fig (5.8): TEM image of sample RPD700D

The first experiment was a polarized scattered light (VV) experiment. The count rate of this experiment was around 10kcps. A typical auto correlation function for sample RPD700D is shown in Fig (5.9).
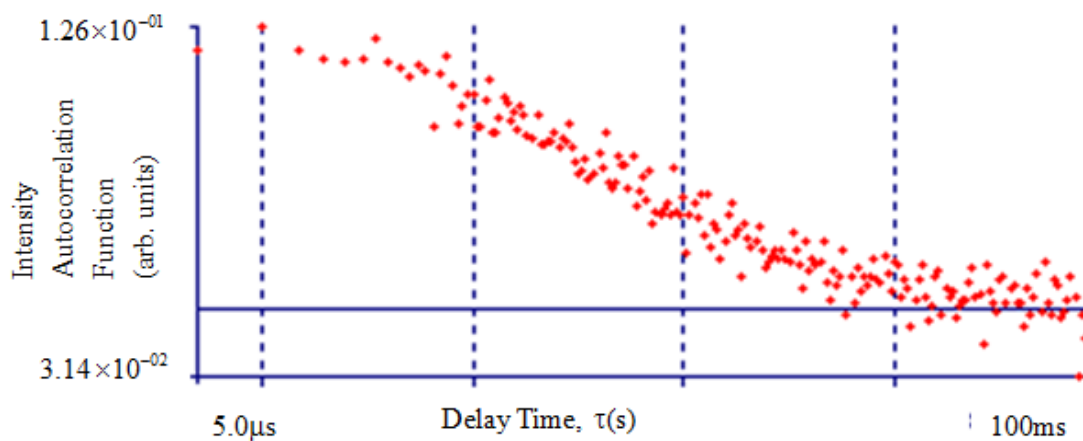
Fig (5.9): The autocorrelation function of polarized experiment for sample RPD700D

43

The relaxation rate intensity (weight) versus relaxation rate graph is shown in Fig (5.8) which was obtained using a double exponential fitting of the autocorrelation function. The summary was also included with the actual graph.
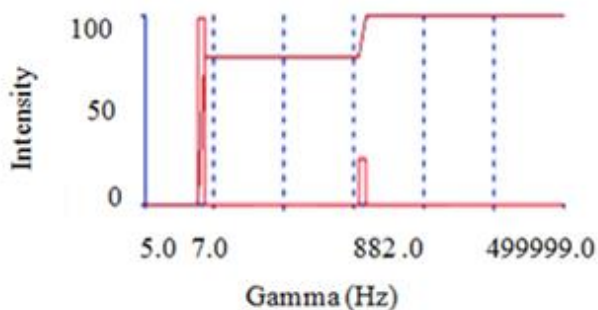
Fig (5.10): Relaxation rate intensity (weight) versus relaxation rate graph for sample RPD700D

The second experiment was a depolarized light scattering (VH) experiment. The count rate of this experiment was around 1.5 kcps, which was 1/7 th times lower than the count rate obtained in polarized light scattering experiment. The auto correlation function of depolarized experiment is shown in Fig (5.10) from which the software was unable to extract any relaxation rate.
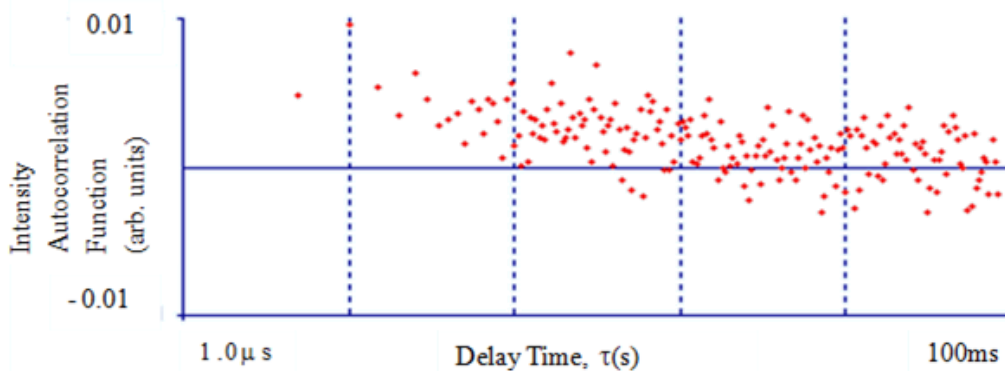
Fig (5.11): Depolarized light (VH) The autocorrelation function for sample RPD700D

Table 5.3 summarizes the results of measurements on sample RPD700D.

Translational relaxation rate Γ_{tr} (Hz)	Mixed relaxation rate Γ_{mix} (Hz) (Polarized)	Mixed relaxation rate Γ_{mix} (Hz) (Depolarized)	Rotational relaxation rate Γ_{rot} (Hz) (Polarized)	Length L (nm)	Aspect Ratio AR	Diameter D (nm)
7	882	-	875	30	1.9	16
4	581	-	577	28	2.0	15
7	597	-	590	37	2.0	13
5	425	-	420	37	2.0	15
4	578	-	573	30	2.0	10
2	714	-	711	21	2.0	13
6	915	-	909	27	2.1	13
4	740	-	735	26	2.0	10
12	998	-	986	37	1.9	11
3	772	-	768	22	2.0	11
4	877	-	873	22	2.0	9
4	857	-	853	22	2.0	11
29	1480	-	1451	48	2.0	10
4	1207	-	1203	18	2.0	15
3	657		654	21	2.0	16
3	1004	-	1000	19	2.0	14
8	1024	-	1016	30	2.0	9
31	1269	-	1238	54	2.0	12
11	1323	-	1312	31	2.1	24
5	778	-	772	28	2.0	12
4	1214	-	1210	18	2.0	13
4	791	-	787	24	2.0	12
14	927	-	912	43	2.0	21
14	723	-	709	48	2.2	21
5	948	-	942	25	2.0	12

Table 5.3: Result of sample RPD700D

5.2.3 Sample RPD 235AD:

This was another sample of bare gold nanorods. The nanorod concentration of this sample in solution was 8.3×10^{10} particle /ml. It was also dispersed in DI water. The published

viscosity and Refractive Index in this case were the same as those for the sample RPD700D. The scattering angle was again 90°, so the scattering wave vector for this nano-rod solution in DI water was also 0.018/nm. The TEM image of sample RPD235AD which was taken in laboratory is shown in Fig (5.12). According this image the distribution of length was 81 ± 9nm and distribution of diameter was 32 ± 3nm.
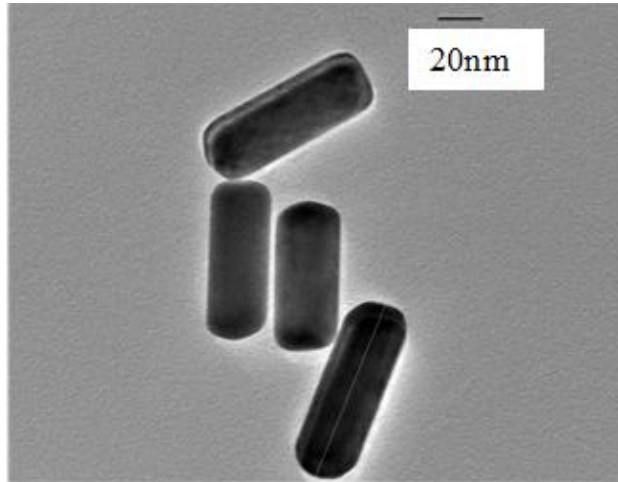
Fig (5.12): TEM image of sample RPD235AD

A typical autocorrelation function for the polarized scattered light intensity (VV) experiment for this sample is shown in Fig (5.13). The count rate was approximately 45 kcps.
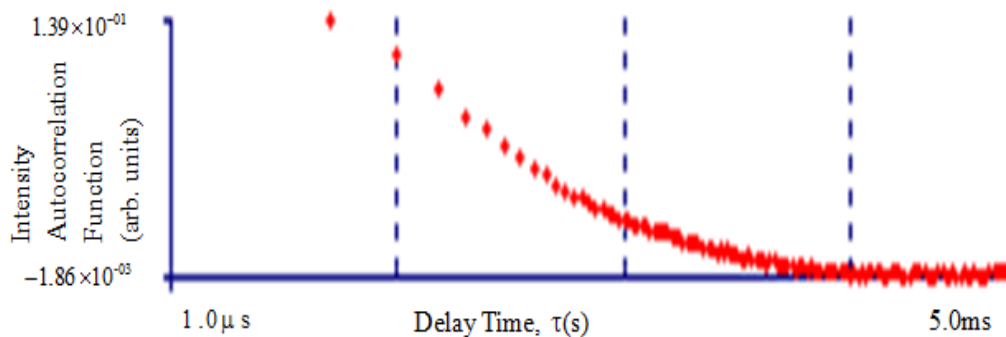
Fig (5.13): Autocorrelation function of polarized light (VV) experiment for sample RPD235AD

A double exponential fitting of the measured autocorrelation function gave the relaxation rate versus relaxation rate intensity graph shown in Fig (5.14).
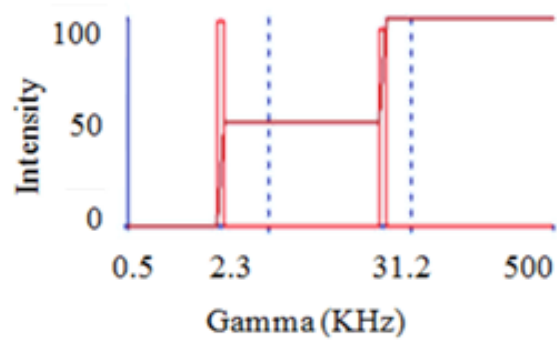
Fig (5.14): Relaxation rate intensity (weight) versus relaxation rate graph for sample RPD235AD

In the depolarized scattered light (VH) experiment, the count rate was around 15kcps, which was 10 times higher than in the preceding depolarized light experiments. The relaxation rates extracted from this measurement were in agreement with those derived from the measurements of mixed relaxation rates in polarized light (VV) experiment. A typical auto correlations function of this experiment is shown in Fig (5.15).
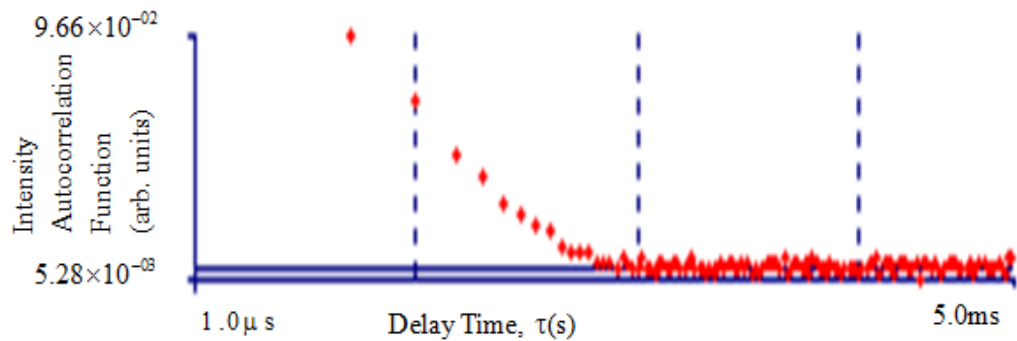
Fig (5.15): Typical autocorrelation function of depolarized light (VH) for sample RPD235AD

The results of all experiments for sample RPD235AD are listed in Table 5.4. The same procedure had been used as that for the other two samples.

Translational relaxation rate Γ_{tr} (KHz)	Mixed relaxation rate Γ_{mix} (KHz) (Polarized)	Mixed relaxation rate Γ_{mix} (KHz) (Depolarized)	Rotational relaxation rate Γ_{rot} (KHz) (Polarized)	Length L (nm)	Aspect Ratio AR	Diameter D (nm)
2	34	29	32	93	4.4	21
2	32	29	30	94	4.2	23
2	28	27	26	94	3.2	29
2	29	29	27	95	3.7	26
2	27	27	25	95	3.2	30
2	33	29	31	96	4.9	20
2	27	26	25	95	3.3	29
2	28	28	26	96	3.8	25
2	33	28	31	93	4.3	22
2	30	27	28	92	3.4	27
2	26	29	24	95	3.1	31
2	29	26	27	96	4.1	24
2	30	28	28	95	4.0	24
3	35	28	33	94	5.0	19
2	29	28	27	95	3.8	25
2	31	30	29	94	3.9	24
2	31	26	29	93	3.8	25
2	27	31	25	98	3.8	26
2	33	27	31	93	4.0	23
2	28	30	26	95	3.7	26
2	32	22	30	95	4.4	22
2	29	29	27	97	4.0	24
2	31	28	29	96	4.4	22
2	29	29	27	96	3.9	25
2	29	30	27	96	3.9	25

Table5.4: The result of sample RPD235AD

In the Table5.5, the length and diameter distribution determined by dynamic light scattering technique were compared with those obtained from transmission electron microscopy. The TEM value provided by manufacturer is shown along with the TEM which was done in the

UA laboratory. The standard deviation was also included with the average length, aspect ratio and diameter. The manufacturer provided TEM length, aspect ratio and diameter of sample 001 were 24 ± 4 nm, 2.5 ± 1.0 and 10 ± 1 nm respectively. Because of insufficient sample repeated TEM image was not taken in laboratory. On the other hand, the DLS average results were 18.2nm, 1.97 and 9.2nm. The standard deviations were not included with these values because of insufficient repeated result. In case of sample RPD700D, the DLS measurement of length, aspect ratio and diameter were 27 ± 8 nm, 2.0 ± 0.1 , 13 ± 3 nm, respectively, and the company provided TEM measurements of these parameters were 32 nm, 3.2 and 10 nm respectively. According to the TEM image done in the UA laboratory the length distribution was 23 ± 8 nm, the aspect ratio distribution was 2.4 ± 1.0 and the diameter distribution was 10 ± 2 nm. The last sample was RPD235AD. According to the DLS measurement the length distribution of this sample was 95.0 ± 1.3 nm, aspect ratio distribution was 4.0 ± 0.1 and diameter distribution was 32.0 ± 3.4 nm. The same parameters using TEM technique by company were 72 nm, 3.2 and 22.5 nm, respectively. On the other hand the TEM (done in the UA laboratory) values of length, aspect ratio and diameter distribution were 80 ± 8 nm, 2.5 ± 0.4 and 25 ± 3 nm respectively.

Sample	Length (nm)			Diameter (nm)		
	DLS	TEM (Manufacturer)	TEM (Lab)	DLS	TEM (Manufacturer)	TEM (Lab)
001	18.2	24 ± 4	NA	9.2	10 ± 1	NA
RPD700D	27.0 ± 8.0	32	23 ± 8	13 ± 3	10	10 ± 2
RPD235AD	95.0 ± 1.3	72	80 ± 8	32.0 ± 3.4	22.5	25 ± 3

Table 5.5: Comparing of DLS result with TEM result

Chapter 6

Conclusion

The purpose of this thesis was to demonstrate that dynamic light scattering technique is a viable technique for determining nanorod size and shape in a fluid medium. This has been demonstrated by measuring, successfully, three nanorod samples. The length, aspect ratio and diameter of three nano-rod samples have been determined by this technique. The results obtained from DLS were also compared with those obtained form TEM. In the experiments, both polarized and depolarized scattered light measurements were carried out. The auto-correlation function of vertically polarized scattered light contains both mixed and translational relaxation rates. The rotational relaxation rate is the (positive) difference of mixed and translational relaxation rates. The decay time and relaxation rates are reciprocals of each other. Since the decay time for rotational movement is smaller than the translational movement, the rotational relaxation rate is higher than the translational relaxation rates. On the other hand the analysis of auto-correlation function of depolarized scattering light yields only the mixed relaxation rate. According to Eqs. 2.52 and 2.53, the mixed relaxation rates determined by polarized and depolarized light experiments should be equal. This prediction has been verified for the sample RPD235AD.

In the case of sample 001 and RPD700D it was not possible to extract the mixed relaxation rate from the depolarized scattering light experiment due to low intensity of depolarized intensity. Since the nanorods in these two samples were smaller than those in sample RPD235AD, both polarized and depolarized scattered light intensities were low because light scattering is directly proportional to the ratio of the fourth power of particle size to wavelength ratio. The depolarized scattered light intensity is even lower because of smaller

50

diameter (smaller aspect ratio). Consequently, the auto correlation function had too large a scatter to fit an exponential reliably to yield any meaningful information that can be used for determining the diameter of nanorods. The experiment was also limited by the available laser power, which could have increased the signal count rate.

The theoretical background presented in this thesis and the experimental procedure based on dynamical light scattering used to extract information about particle size and can be applied for characterizing other nano particle of anisotropic shape. This method can also be used to determine the size distribution of nanoparticles. Indeed, the information in Figs. (5.6), (5.10) and (5.14) can be de-convoluted to obtain size distribution as the size and relaxation rates are related.

Finally, light scattering signal gets weaker as the size of scatterers becomes smaller. It is strongest for particles of size comparable to the wavelength of light. So for very small particles, dynamical light scattering is not expected to be yield meaningful size information due to small signal. Increasing the light intensity may increase the signal but may result in heating of the sample. Using a laser with shorter wavelength may also increase scattering as it is inversely proportional to the fourth power of wavelength.

The limits of dynamical light scattering in terms of incident light power, wavelength, and particle size were not quantified because of the limitations on available light power and particle size samples. The experiments described here showed that dynamical light scattering is an inexpensive and has the potential to be an effective technique for analyzing particle shapes and sizes down to a few nanometers and aspect ratios as small as 1.9 for certain types of particles at a lower cost. For more complicated shapes or aspect ratios close to one, it may yield only average size information. To realize the full potential of DLS and fully characterize its limitations as a technique for determining shape and size will require further studies.

References:

1. Benjamin Chu, *Laser Light Scattering* (Academic Press Inc., 1991) pp 13-16, 35-38.

2. Bruce J. Berne and Robert Pecora, *Dynamic Light Scattering* (John Wiley & Sons, Inc., 1976) pp 24-32, 53-60.

3. Albert Einstein, *Investigation on the Theory of the Brownian Movement* (Dover, New York, 1926).

4. Michael Glidden and Martin Muschol,"Characterizing Gold Nanorods in Solution Using Depolarized Dynamic Light Scattering," J. Phys. Chem., 116, 8128−8137 (2012).

5. Jessica Rodrigue-Fernandez, Jorge Perez-Juste, Luis M. Liz-Marzan, and Peter R. Lang, "Dynamic Light Scattering of Short Au Rods with Low Aspect Ratio," J. Phys. Chem. 111, 5020-5025 (2007).

6. Hideatsu Maeda, Nobuhiko Saito, "Spectral Distribution of the Light Scattered from Rodlike Macromolecules in Solution. II The Effect of optical Anisotropy," Polymer Journal 4, pp 309-315 (1973).

7. Shutang Chen, Samir V. Jenkins, Jing Tao, Yimei Zhu, Jingyi Chen, "Anisotropic Seeded Growth of Cu−M (M = Au, Pt, or Pd) Bimetallic Nanorods with Tunable Optical and Catalytic Properties", J. Phys. Chem. 117, 8924-8932 (2013)

Appendix A: Description of research for popular publication

Mega savings of tiny particle sizing by laser light!

To determine the size of particle researchers have been spending a lot of money behind traditional Transmission electron microscopy or TEM technique. But now for the first time so called Dynamic Light Scattering Technique has been used to characterize these tiny particles by researcher which is a cheaper technique. In addition with this it allows the researcher to determine particle size under realistic conditions that involve their suspension in a fluid medium. So research on biomolecule will be really boosted by this new technology.

A traditional inexpensive He:Ne laser is sufficient as a light source. The size of particle is extracted from the scattered light due to the particle and laser light interaction and analyzed by a photomultiplier. Besides the size of particle molecular weight, diffusion coefficient, temperature dependency etc can be also determined by this technique. The sizes of nanosphere and nanorod samples were successfully determined by this technique. Recently University of Arkansas physics Professor Dr. Surendra P. Singh and his Masters student Marzia Zaman have done most updated research on this technique. They have measured nanorod of aspect ratio 1.9. So far this is the smallest aspect ratio determined by this technique. Marzia says, "My next plan is to measure the particle of anisotropic shaped". Based on this research it can be assumed that in near future this technique will be used commercially to characterize nanoparticle.

Sample Name	Length (nm)		Diameter (nm)	
	DLS	TEM	DLS	TEM
001	18.2	24±4	9.2	10±1
RPD700D	27.0±8.0	23±8	13±3	10±2
RPD235AD	95.0±1.3	80±8	32.0±3.4	25±3

Nanorod sizing In a Recent research, size of bare Gold and Gold-Copper alloy nanorod has been determined by DLS technique. The smallest aspect ratio determined by this research is around 2 which is very small.

53

Appendix B: Executive summary of newly created intellectual property

Dynamical light scattering (DLS) is a technique for particle sizing. Its use for determining nano-particle shape is relatively recent. While the research in this thesis was not the first to demonstrate its usefulness in determining the shape (aspect ratio), we have been able to extend the range of its applicability. The following list summarizes principal intellectual property outcomes of this research project.

1. Nanorods with aspect ratio 1.9 (smaller by a factor of 2 compared to previous studies) have been measured with the Dynamic Light Scattering Technique.

2. For the same aspect ratio, the Dynamic Light Scattering Technique (DLS) cannot be used for all nanorod sizes; low depolarization light scattering intensity for very short nanorods prevents a reliable estimate for the smaller dimension of the rod.

3. This technique can be used to determine the size distribution of particles. Although this information is not presented in the thesis, since the focus was on determining the shape or the aspect ratio, it is an outcome of the analysis of the experiment.

Appendix C: Potential patent and commercialization aspects of listed intellectual property items

C.1 Patentability of intellectual property

The three items listed were considered first from the perspective of whether or not the item could

be patented.

1. Characterizing nanorod of lower aspect ratio can be patented.

2. The Dynamic Light Scattering Technique cannot be patented but the lower limit of nanorod size under which this technique cannot be applicable can be determined and patented after doing more experiment on some other short nanorod samples.

3. The size distribution measurement is actually average size distribution not the ultimate so cannot be patented.

C.2 Commercialization prospects

The three items listed were then considered from the perspective of whether or not each item should be patented.

1. Characterizing nanorod of lower aspect ratio should be patented because for a realistic (in a fluid medium) characterization of nanorod with smaller aspect ratio, this is the only technique which can be commercialized.

2. The determining of lower limit of the size under which the DLS technique is not applicable should be added to the previous patent.

3. Not patentable as mentioned in C.1.

C.3 Possible prior disclosure of IP

The following items were discussed in a public forum or have published information that could impact the patentability of the listed IP.'

1. The results of DLS measurement on nanorod of as small an aspect ratio as 1.9 have not been published in any forum.

2. The problems associated with shorter nanorod have not been discussed in any forum.

3. The prediction of experiment on size distribution of nanoparticle by DLS technique has not been published yet.

Appendix D: Broader impact of research

D.1 Applicability of research methods to other problems

The theoretical background presented in this thesis and the experimental procedure based on dynamical light scattering used to extract information about particle size and can be applied for characterizing other nano particle of anisotropic shape. This method can also be used to determine the size distribution of nanoparticles. The reactivity of nanoparticle can be also measured by doing this experiment at different concentration of solution.

D.2 Impact of research results on U.S. and global society

This research has no direct impact on US and global society but obviously in science and technology, the study on Dynamic Light Scattering Technique is a potentially useful technique for charactering nanoparticles in a relatively inexpensive and realistic way.

D.3 Impact of research results on the environment

The experiment did not have any harmful impact on the environment. A He:Ne laser light source was used so precaution should be taken to prevent the eyes from exposure to laser radiation though the power of laser is low. Special care is needed to use and dispose off two materials: Decalin and Sulfuric acid in accordance with the chemical safety rules.

Appendix E: Microsoft project for MS MicroEP degree plan
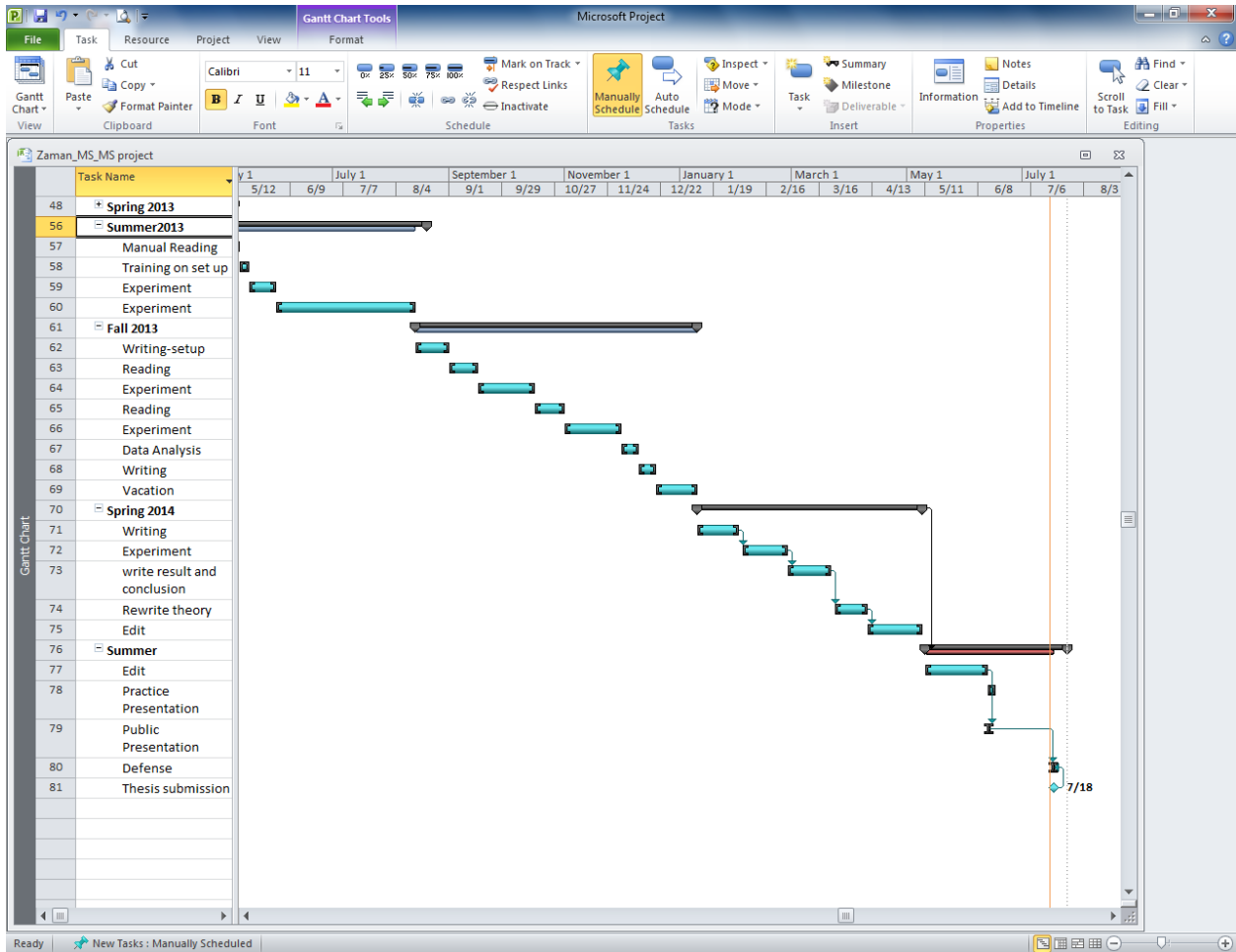
Appendix F: Identification of all software used in research and thesis generation

Computer #1:
      Model Number: Dell Dimension 8300
      Location: Physics Library
      Owner: University of Arkansas, Physics Department
Software #1:
      Name: Microsoft Office 2007
      Purchased by: UA Physics Dept.
Software #2:
      Name: BI-9000AT Digital Autocorrelator
      Purchased by: Dr. Surendra P. Singh